(3100, Applied Biosystems) with the BigDye terminator cycle sequencing kit (Applied Biosystems). When mutations were found by direct sequencing, the fragments were cloned into a pTOPO vector (Invitrogen) and then transfected into the *E. coli* strain DH5A. At least four recombinant colonies were selected, and plasmid DNA samples were prepared by using the QIAprep Spin Miniprep kit (Qiagen). Cloned fragments were sequenced to confirm the mutation of the *NPM1* gene.

Total RNA was harvested from purified CD34-positive cells by using an RNeasy minikit (Qiagen). cDNA synthesis was undertaken by using an oligo(dT) primer with the PrimeScript II first strand cDNA synthesis kit (Takara, Shiga, Japan). These cDNA molecules were measured by RQ-PCR with the primers listed under "RQ-PCR."

RQ-PCR—RQ-PCR was performed by using a LightCycler TaqMan Master kit (Roche Applied Science) following the manufacturer's instructions. Twenty microliters of Universal ProbeLibrary probes (Exiqon, Vedbaek, Denmark) were added in the final reaction. Primers designed by using the Universal ProbeLibrary Assay Design Centre (available on the Roche Applied Science Web site) were synthesized by Sigma. PCR amplification was performed by using a LightCycler 350S instrument (Roche Applied Science). Thermal cycling conditions comprised 2 min at 40 °C and 10 min at 95 °C, followed by 45 amplification cycles at 95 °C for 10 s, 60 °C for 30 s, and 72 °C for 1 s and then a 40 °C cooling cycle for 30 s. Specific primers and probes were as follows: for *HDM2*, forward (5′-TCTGATAGTATTTCCCTTTCCTTTG-3′), reverse (5′-TGTTCACTTACACCAGCATCAA-3′), and probe (5′-CGCCACTTTTTCTCTGCTGATCCAGG-3′); for human *MEF/ELF4*, forward (5′-TGGAGACTCTCAGGGTCGAAA-3′), reverse (5′-AAGCAACGGGATGGATGAT-3′), and probe (5′-TCACAGCTGGGAACACAGAG-3′); and for human *G6PDH*, forward (5′-AAGCAACGGGATGGATGAT-3′), reverse (5′-TCACAGCTGGGAACACAGAG-3′), and probe (5′-CGCCACTTTTTCTCTGCTGATCCAGG-3′).

Statistical Analyses—Comparisons of patient characteristics between two groups were performed with the Wilcoxon test. The results of *in vivo* experiments are presented as the mean ± S.D. of three independent experiments and compared by using one-way analysis of variance followed by Scheffe's multiple comparison test. A p value of 0.05 was considered statistically significant.

RESULTS

Identification of MEF/ELF4-binding Protein—To identify the proteins that bind to MEF/ELF4, we performed the tandem affinity purification (TAP) procedure and analyzed the amino acid sequence of the protein complex, thereby identifying 25 proteins (including NPM1). NPM1 is essential for embryonic development and is frequently translocated or mutated in hematological malignancies (24). Therefore, we decided to focus on the interaction between NPM1 and MEF/ELF4.

Wt-NPM1 Interacts with MEF/ELF4 in Vivo and in Vitro—To determine if Wt-NPM1 interacts with MEF/ELF4 in human cells, we transfected 293T cells with FLAG-MEF/ELF4 and V5-Wt-NPM1 expression plasmids and performed immunoprecipitations with mouse monoclonal anti-FLAG or anti-V5 antibody. As shown in Fig. 1*A*, FLAG-MEF/ELF4 protein co-precipitated with V5-Wt-NPM1 by the anti-V5 antibody (*lane 1*) but not by the isotype-matched control (*lane 2*). In reciprocal experiments, V5-Wt-NPM1 protein co-precipitated with FLAG-MEF/ELF4 protein by the anti-FLAG antibody (*lane 3*). These results showed the *in vivo* interaction between Wt-NPM1 and MEF/ELF4. To ascertain whether Wt-NPM1 protein interacted directly with MEF/ELF4, an *in vitro* association assay with biotin-labeled *in vitro*-translated Wt-NPM1 and bacterially recombinant His-MEF/ELF4 fusion protein was performed (Fig. 1*B*). Biotin-labeled Wt-NPM1 bound to His-MEF/ELF4 (*lane 1*) but not to His alone (*lane 2*). These results demonstrated that His-MEF/ELF4 bound directly to Wt-NPM1.

To characterize the region of Wt-NPM1 that binds MEF/ELF4, five distinct GST-NPM1 proteins were prepared (Fig. 1*C*). GST pull-down assays (Fig. 1*D* (*a*)) and His tag pull-down assays (Fig. 1*D* (*b*)) revealed that the N-terminal region of NPM1 (the F1, F2, and F3 fragments that contain the oligomerization domain) bound to His-MEF/ELF4, unlike the C-terminal region of NPM1 (F4 and F5).

Wt-NPM1 Interferes with MEF/ELF4 Binding to Target DNA Sequences—To assess the direct role of Wt-NPM1 in MEF/ELF4 action, we undertook EMSA. His-MEF/ELF4 bound to the APET probe (1), but no band was observed with His, GST, or GST-NPM1 (Fig. 2). The shifted band of MEF/ELF4 was diminished when the APET competitor was added to the reaction mixture. When Wt-NPM1 was added to the reaction mixture, the shifted band containing MEF/ELF4 was diminished. These results implied that Wt-NPM1 inhibits the DNA binding of MEF/ELF4 DNA through direct interactions.

Wt-NPM1 Inhibits, whereas Mt-NPM1 Enhances, MEF/ELF4-dependent Transcriptional Activity—To study the functional relevance of the physical interaction between MEF/ELF4 and Wt-NPM1, we transfected pcDNA/MEF/ELF4 in combination with pcDNA/Wt-NPM1 and examined the activity of the APET promoter construct (1) in 293T cells (Fig. 3*A*). As reported previously, MEF/ELF4 activated the APET promoter by ~159-fold. Co-expression of Wt-NPM1 with MEF/ELF4 led to a significant decrease in luciferase activity. Similar data were obtained by using COS7 cells (Fig. 3*B*) and a human leukemia cell line, U937 (Fig. 3*C*).

Having shown that NPM1 expression attenuated the transcriptional activity of MEF/ELF4 in leukemia cells, we next assessed whether the inhibition of Wt-NPM1 expression *in vivo* enhanced MEF/ELF4-dependent transcriptional activity. The siRNA directed against Wt-NPM1 in 293T cells suppressed the expression of Wt-NPM1 protein by 60–70% (Fig. 3*D*). Transient transfections were performed by using NPM1-knockdown 293T cells with pcDNA/MEF/ELF4 and pGL4/APET reporter plasmids. A luciferase assay revealed that MEF/ELF4-dependent transcriptional activity was significantly elevated in Wt-NPM1-knockdown cells by 1.8-fold (Fig. 3*E*). These results implied that Wt-NPM1 functioned as an inhibitor of MEF/ELF4.

Mutated nucleophosmin (Mt-NPM1) has been found in 50% of adult AML patients with normal karyotypes (15). It has been suggested that the mutation is a critical event for leukemogen-

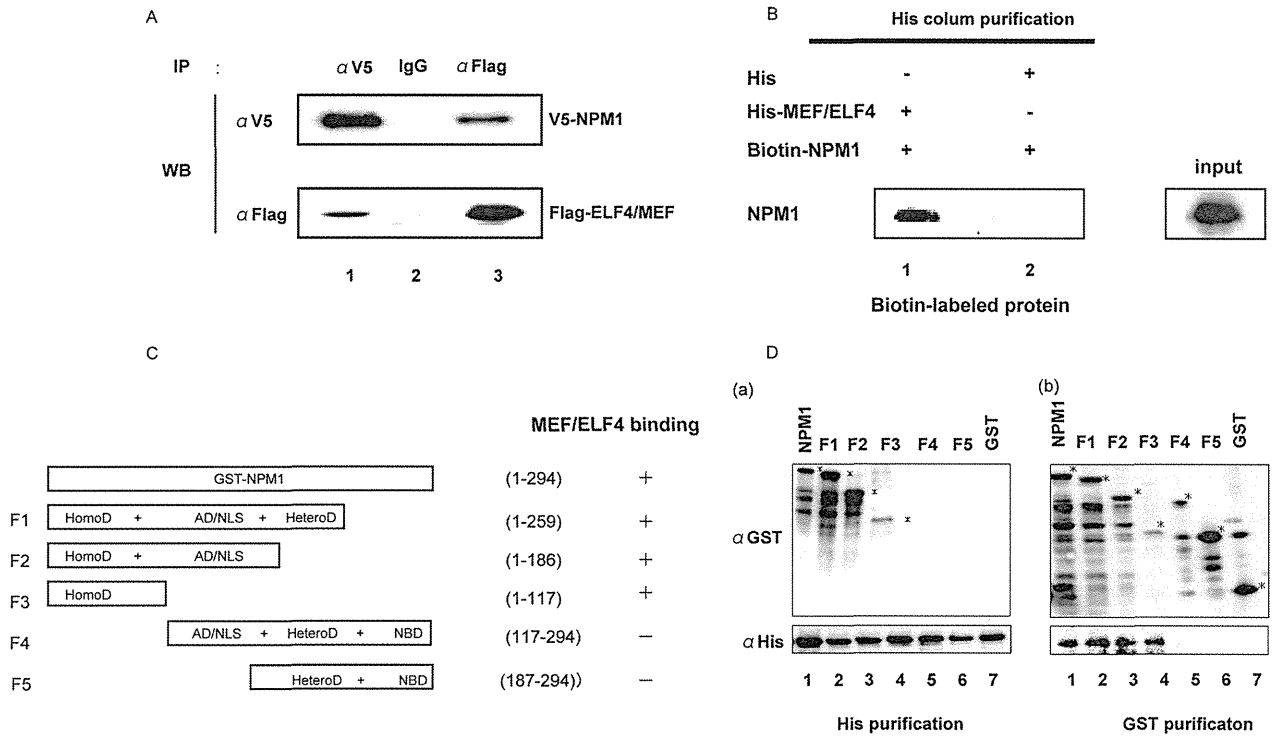

FIGURE 1. **NPM1 interacts with MEF/ELF4.** *A*, 293T cells were transfected with the indicated expression plasmids. After 48 h, cell lysates were immunoprecipitated (*IP*) with anti-FLAG and anti-V5 antibodies. Immunoprecipitates were analyzed by 10% SDS-PAGE and subjected to immunoblotting (*WB*) with anti-V5 antibody (*top row*) or anti-FLAG antibody (*bottom row*). *B*, MEF/ELF4 interacts directly with NPM1 *in vitro*. *In vitro* association assays were undertaken by incubating His-MEF/ELF4 fusion protein immobilized by using a His-column with biotin-labeled MEF/ELF4 (*lane 1*). His alone was incubated with biotin-labeled NPM1 (*lane 2*) as a control. *C*, NPM1 structure and the relative binding of MEF/ELF4 (*schematic*). *HomoD*, homodimerization domain, residues 1–117; *AD/NLS*, acidic domain/nuclear localization sequence, residues 117–187; *HeteroD*, heterodimerization domain, residues 187–259; *NBD*, nucleic acid binding domain, residues 259–294. *D*, the N-terminal portion of NPM1 is the MEF/ELF4-interacting domain. Bacterially expressed and purified GST, GST-NPM1, and GST-NPM1 mutants with deletions were mixed with bacterially expressed and purified His or His-MEF/ELF4 protein. Recombinant proteins were subjected to His or GST affinity columns, followed by immunoblotting with anti-GST or anti-His antibodies. *a*, the reactive samples were subjected to analyses on a His affinity column followed by immunoblotting with anti-His antibodies (*bottom left*) or with anti-GST antibodies (*top left*). *b*, the reactive samples were subjected to GST affinity columns, followed by immunoblotting with anti-GST antibodies (*top right*) or with anti-His antibodies (*bottom right*).

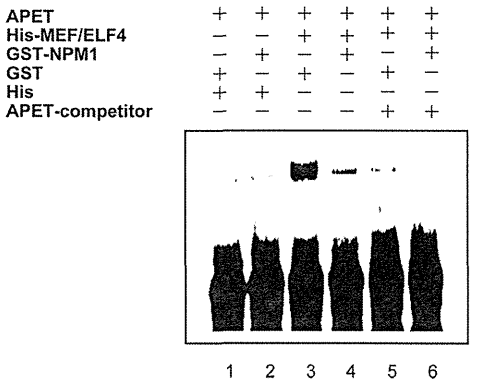

FIGURE 2. **EMSA with recombinant His-MEF/ELF4, His, GST, and GST-Wt-NPM1.** His-MEF/ELF4 was incubated with GST and GST-Wt-NPM1 at room temperature prior to EMSA by using a biotin-conjugated APET probe (*lanes 1–4*). An excess amount of unlabeled APET competitor was added to the reaction mixtures (*lanes 5* and *6*).

esis. To determine the effect of Mt-NPM1 on the transcription-activating properties of MEF/ELF4, we transfected pcDNA/MEF/ELF4 in combination with pcDNA/Mt-A-NPM1, pcDNA/Mt-I-NPM1, or pcDNA/Mt-J-NPM1 and then examined the activity of the APET promoter construct in 293T cells (Fig. 3*F*). Co-expression of Mt-NPM1 with MEF/ELF4 led to a 315-fold increase in luciferase activity. Similar data were obtained with COS7 (Fig. 3*G*) and U937 (Fig. 3*H*) cells. To show the effect of the coexistence of both Wt- and Mt-NPM1, we transfected 293T cells with various amounts of plasmids that expressed Wt-NPM1 and Mt-A-NPM1. The expression of Mt-NPM1 enhanced MEF/ELF4-dependent APET promoter activation in a dose-dependent manner, even in the presence of Wt-NPM1 (Fig. 3*I*). Taken together, our results suggest that Wt-NPM1 has an inhibitory effect, whereas Mt-NPM1 has enhancing effect, on the function of MEF/ELF4.

Mt-NPM1 Does Not Interact with MEF/ELF4 in Vivo—Because the mutated region of Mt-NPM1 was located outside the domain responsible for interaction with MEF/ELF4, we hypothesized that Mt-NPM1 might bind to MEF/ELF4. To test this hypothesis, we transfected 293T cells with FLAG-MEF/ELF4 and V5-Mt-A-NPM1 expression plasmids and performed immunoprecipitations with mouse monoclonal anti-FLAG or anti-V5 antibody. Contrary to our expectations, as shown in Fig. 4, FLAG-MEF/ELF4 protein and V5-Wt-A-NPM1 did not co-precipitate with each other (Fig. 4). These results showed that there is little *in vivo* interaction between Mt-A-NPM1 and MEF/ELF4.

Localization of MEF/ELF4 Is Unaffected by Mt-NPM1—Having shown that Mt-NPM1 enhances the transcriptional activity of MEF/ELF4, we next assessed whether Mt-NPM1 dislocates

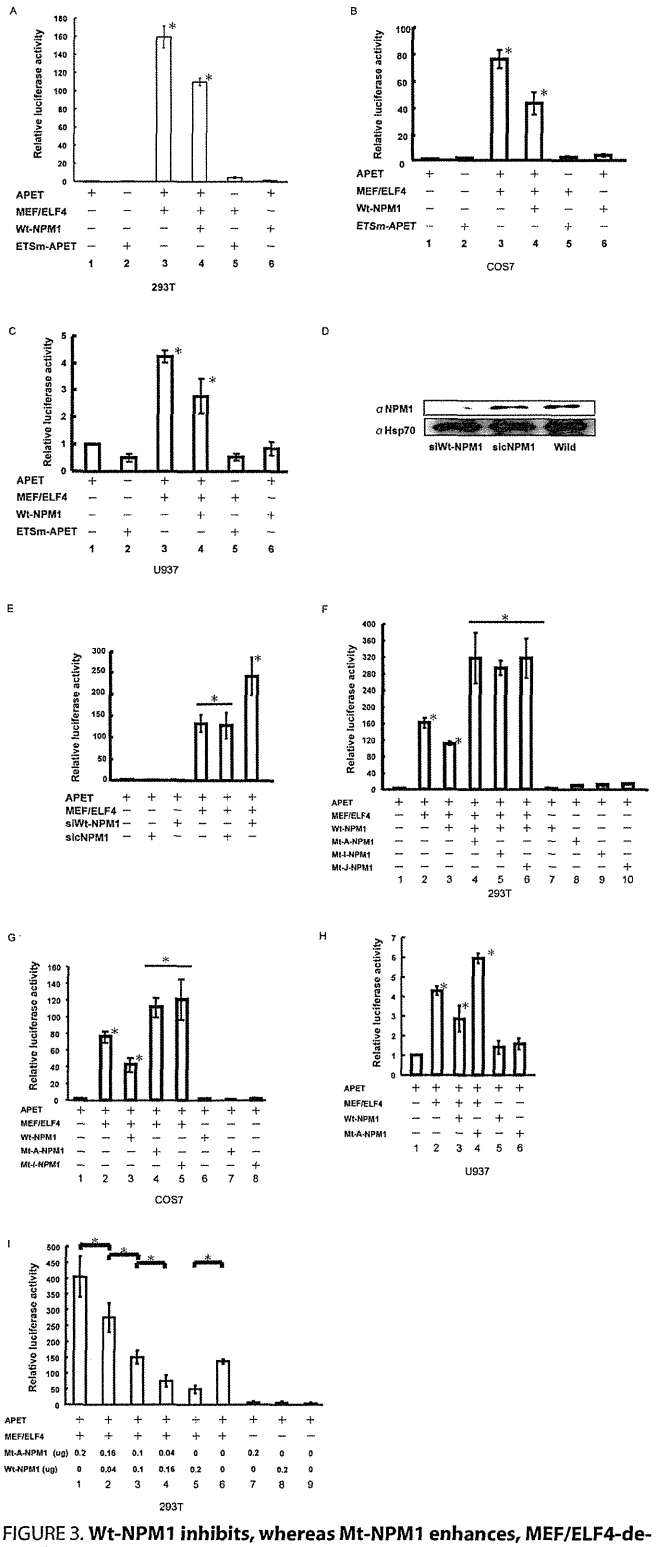

FIGURE 3. **Wt-NPM1 inhibits, whereas Mt-NPM1 enhances, MEF/ELF4-dependent APET promoter transactivation.** 293T human kidney (*A*), COS7 monkey kidney (*B*), and U937 human hematological (C) cell lines were co-transfected with the luciferase reporter gene of an artificial MEF/ELF4 target promoter (APET) and effector genes. The target promoter and effector genes were as follows: pGL4/APET (*lane 1*); pGL4/ETSm-APET (*lane 2*); pGL4/APET and pcDNA/MEF/ELF4 (*lane 3*); pGL4/APET, pcDNA/MEF/ELF4, and pcDNA/Wt-NPM1 (*lane 4*); pGL4/ETSm-APET and pcDNA/MEF/ELF4 (*lane 5*); and pGL4/APET and pcDNA/Wt-NPM1 (*lane 6*). Luciferase activity by pGL4/APET alone was assigned a value of 1.0. The analysis was performed in triplicate assays, and the results were reproducible. The results are shown as the mean ± S.D. (*error bars*). *, $p < 0.05$. *D*, 293T cells transduced with siRNA encoding vector (siWt-NPM1) were harvested 72 h after transduction for Western blotting. Hsp90 is shown as a control. *sicNPM1*, control siRNA non-relevant to the expression of NPM1; *Wild*, without transduction. *E*, 293T cells were co-transfected with the luciferase reporter plasmid (pGL4/APET), expression plasmid (pcDNA MEF/ELF4), and siWt-NPM1 gene (pcDNA/siRNA-Wt-NPM1) or control. Luciferase activity by pGL4/APET alone was assigned a value of 1.0. The analysis was performed in triplicate assays, and the results were reproducible. The results are shown as the mean ± S.D. *, $p < 0.05$. *F*, 293T cells were co-transfected with the luciferase reporter gene of an artificial MEF/ELF4 target promoter and effector genes. Target promoter and effector genes were as follows: pGL4/APET (*lane 1*); pGL4/APET and pcDNA/MEF/ELF4 (*lane 2*); pGL4/APET, pcDNA/MEF/ELF4, and Wt-NPM1 (*lane 3*); pGL4/APET, pcDNA/MEF/ELF4, and Mt-A-NPM1, Mt-I-NPM1, or Mt-J-NPM1 (lanes 4–6, respectively); and pGL4/APET and pcDNA/Wt-NPM1, Mt-A-NPM1, Mt-I-NPM1, or Mt-J-NPM1 (lanes 7–10, respectively). Luciferase activity by pGL4/APET alone was assigned a value of 1.0. The analysis was performed in triplicate assays, and the results were reproducible. The results are shown as the mean ± S.D. *, $p < 0.05$. *G*, COS7 cells were co-transfected with the luciferase reporter gene of an artificial MEF/ELF4 target promoter and effector genes. The target promoter and effector genes were as follows: pGL4/APET (*lane 1*); pGL4/APET and pcDNA/MEF/ELF4 (*lane 2*); pGL4/APET, pcDNA/MEF/ELF4, and Wt-NPM1 (*lane 3*); pGL4/APET, pcDNA/MEF/ELF4, and Mt-A-NPM1 or Mt-I-NPM1 (*lanes 4* and *5*, respectively); and pGL4/APET and pcDNA/Wt-NPM1, Mt-A-NPM1, or Mt-I-NPM1 (*lanes 6–8*, respectively). Luciferase activity by pcDNA/APET alone was assigned a value of 1.0. The analysis was performed in triplicate assays, and the results were reproducible. The results are shown as the mean ± S.D. (*, $p < 0.05$). *H*, U937 cells were co-transfected with the luciferase reporter gene of an artificial MEF/ELF4 target promoter and effector genes. Target promoter and effector genes were as follows: pGL4/APET (*lane 1*); pGL4/APET and pcDNA/MEF/ELF4 (*lane 2*); pGL4/APET, pcDNA/MEF/ELF4, and Wt-NPM1 (*lane 3*); pGL4/APET, pcDNA/MEF/ELF4, and Mt-A-NPM1 (*lane 4*); and pGL4/APET and pcDNA/Wt-NPM1 or Mt-A-NPM1 (*lanes 5* and *6*, respectively). Luciferase activity by pcDNA/APET alone was assigned a value of 1.0. The analysis was performed in triplicate assays, and the results were reproducible. The results are shown as the mean ± S.D. *, $p < 0.05$. *I*, 293T cells were co-transfected with 0.1 μg of the luciferase reporter gene of an artificial MEF/ELF4 target promoter (*lanes 1–9*) and 0.1 μg of effector genes (pcDNA/MEF/ELF4) (*lanes 1–6*). The effector genes were as follows: 0.2 μg of Mt-A-NPM1 (*lane 1*); 0.16 μg of Mt-A-NPM1 and 0.04 μg of Wt-NPM1 (*lane 2*); 0.1 μg of Mt-A-NPM1 and 0.1 μg of Wt-NPM1 (*lane 3*); 0.04 μg of Mt-A-NPM1 and 0.16 μg of Wt-NPM1 or 0.2 μg of Wt-NPM1 (*lanes 4 and 5*, respectively); none (*lane 6*); pGL4/APET and 0.2 μg of Mt-A-NPM1 (*lane 7*); pGL4/APET and 0.2 μg of Wt-NPM1 (*lane 8*); and pGL4/APET (*lane 9*). Luciferase activity by pGL4/APET alone was assigned a value of 1.0. The analysis was performed in triplicate assays, and the results were reproducible. The results are shown as the mean ± S.D. *, $p < 0.05$.

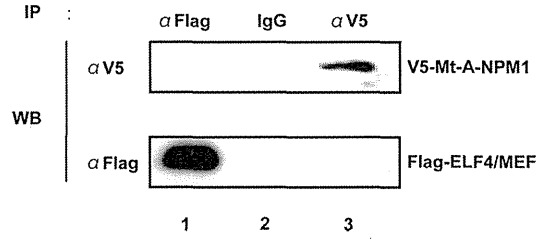

FIGURE 4. **Mt-A-NPM1 does not interact with MEF/ELF4 *in vivo*.** 293T cells were transfected with the indicated expression plasmids. After 48 h, cell lysates were immunoprecipitated (*IP*) with anti-FLAG and anti-V5 antibodies. Immunoprecipitates were analyzed by 10% SDS-PAGE and subjected to immunoblotting (*WB*) with anti-V5 antibody (*top row*) or anti-FLAG antibody (*bottom row*).

MEF/ELF4 into the cytoplasm. We transiently co-transfected a MEF/ELF4-GFP fusion protein vector together with the pcDNA/V-Wt-NPM1 or pcDNA/V-Mt-A-NPM1 expression vector into 293T cells. Wt-NPM1 protein and MEF/ELF4 localized to the nucleus (Fig. 5*A* (*a*)), whereas Mt-A-NPM1 protein localized to the cytoplasm (Fig. 5*A* (b)). Contrary to our expectations, the presence of Mt-A-NPM1 did not affect the subcellular distribution of MEF/ELF4. Western blot analysis of MEF/

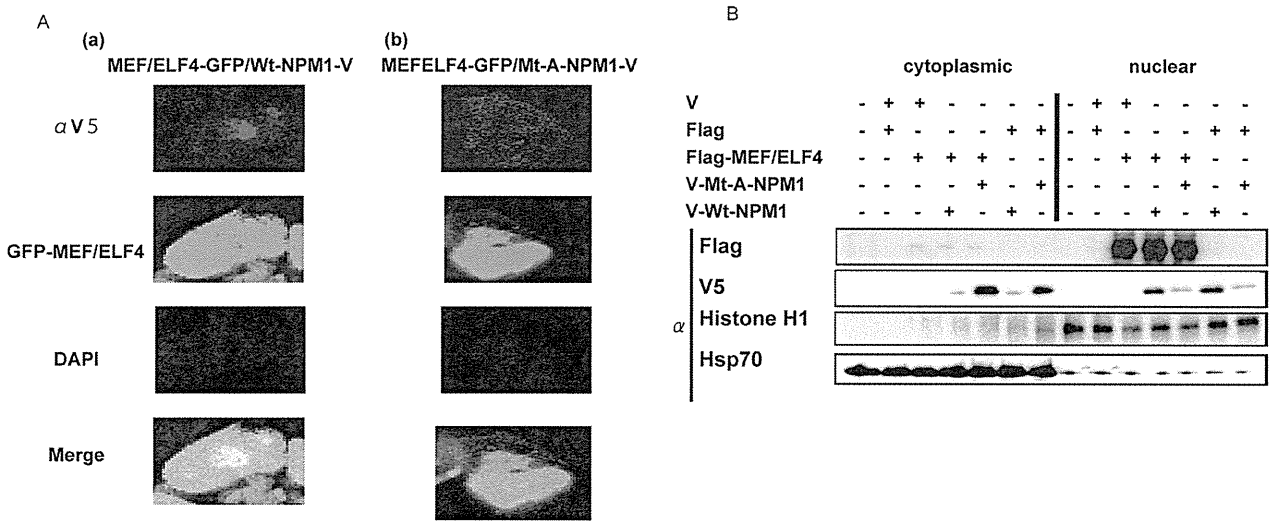

FIGURE 5. **Localization of MEF/ELF4 was unaffected by the mutation of NPM1.** *A*, 293T cells were transfected with the GFP-MEF/ELF4 fusion protein expression vector and pcDNA/V-Wt-NPM1 (*a*) or pcDNA/V-Mt-A-NPM1 (*b*). Forty-eight hours after transfection, cells were fixed and immunofluorescence-stained with anti-V tag antibody. *B*, Western blotting of FLAG-MEF/ELF4 subcellular distribution in 293T cells co-transfected with pFLAG-MEF/ELF4 and pcDNA/V-Wt-NPM1 or pcDNA/V-Mt-A-NPM1. Purity of the subcellular fractions was assessed by blotting with histone H1 (nuclear extraction) and Hsp70 (cytoplasmic extraction).

ELF4 and Wt- or Mt-NPM1 in nuclear and cytoplasmic proteins confirmed the nuclear localization of MEF/ELF4 even with Mt-NPM1 (Fig. 5*B*).

Wt-NPM1 Inhibits, whereas Mt-NPM1 Enhances, the Oncogenic Activity of MEF/ELF4—The overexpression of MEF/ELF4 in NIH3T3 cells increases the growth rate, enhances colony formation in soft agar, and promotes tumor formation in nude mice (10). To determine the effects of the interaction of NPM1 with MEF/ELF4 on cell behavior, we assessed the anchorage-independent growth of NIH3T3 cells after co-transfection of MEF/ELF4 with Wt-NPM1 or Mt-A-NPM1. Compared with NIH3T3 transfected with only MEF/ELF4, Wt-NPM1-coexpressing cells showed reduced anchorage-independent growth, whereas Mt-A-NPM1-coexpressing cells exhibited increased growth (Fig. 6).

MEF/ELF4 Binds to the HDM2 Promoter and Activates Its Expression—In murine cells, MEF/ELF4 binds directly to the Mdm2 promoter, thereby promoting *Mdm2* expression (12). To ascertain whether MEF/ELF4 also directly regulates the promoter activity of *HDM2* (the human analog of Mdm2), we scrutinized the DNA sequence of the *HDM2* gene and found a conserved putative MEF/ELF4 binding site in the P2 promoter (Fig. 7*B*). To establish the association of MEF/ELF4 with the HDM2 promoter, we performed a ChIP assay with nuclear lysates from 293T cells expressing FLAG-MEF/ELF4. Immunoprecipitation with the FLAG antibody (but not with the control IgG) and subsequent PCRs revealed the recruitment of overexpressed MEF/ELF4 to the promoter region of the HDM2 gene (Fig. 7*A*). The luciferase assay revealed that MEF/ELF4 strongly transactivated the wild-type HDM2 promoter (Fig. 7, *B* (*a*) and *C*) and that the effect was abrogated by mutation of the ETS site (−122 to −82) (Fig. 7, *B* (*b*) and *C*). Compared with Wt-NPM1, the expression of Mt-A-NPM1 in 293T cells enhanced the association of MEF/ELF4 with the HDM2 promoter, as detected by ChIP analysis (Fig. 7*D*). Taken together, these findings suggest that Mt-NPM1 up-regulates HDM2 transcription

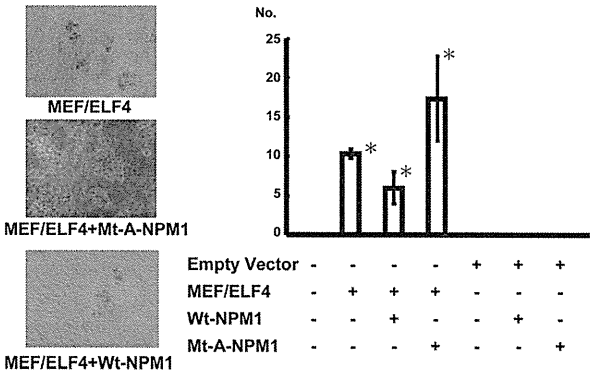

FIGURE 6. **Mt-NPM1 stimulates MEF/ELF4-induced hyperproliferation and transformation.** NIH3T3 cells transfected with various combinations of expression plasmids were plated in soft agar on 60-mm dishes and incubated for 2 weeks. *A*, microscopy of MEF/ELF4-transfected NIH3T3 cells with Wt-NPM1 or Mt-A-NPM1. *B*, the average number of colonies of three independent experiments with S.D. (*error bars*). *, $p < 0.05$.

by increasing the recruitment of MEF/ELF4 to the HDM2 promoter by dislocating Wt-NPM1 that interferes with its binding to the promoter.

Higher Levels of HDM2 mRNA in Clinical Samples from AML Patients with Mt-NPM1 and Higher MEF/ELF4 Expression—To determine the possible clinical relevance of MEF/ELF4, NPM1, and HDM2 in AML patients, we examined the mRNA levels of each in CD34-positive leukemic blasts from 22 AML patients with normal karyotypes. Fourteen patients had Wt-NPM1, and eight patients had Mt-A-NPM1. There was no significant difference between the clinical characteristics of the Wt-NPM1 group and those of the Mt-NPM1 group (Table 1). Samples from the Mt-NPM1 group had significantly higher levels of HDM2 expression as compared with the Wt-NPM1 group ($p = 0.009$) (Fig. 8*A*). In addition, patients with high expression levels of MEF/ELF4 (the MEF/ELF4-H group) had significantly higher HDM2 expression than patients with low expression

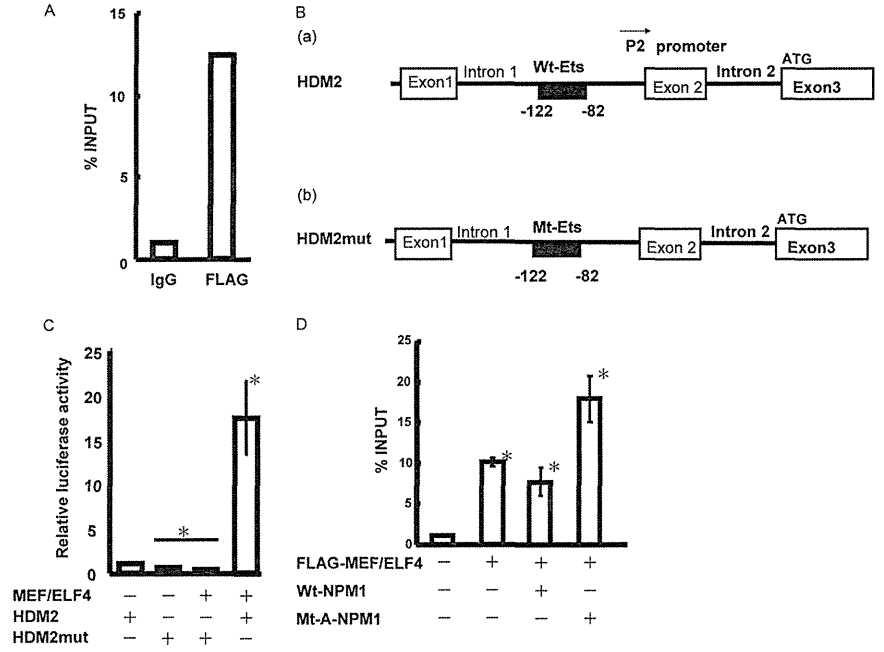

FIGURE 7. **MEF/ELF4 transactivates the HDM2 promoter.** *A*, MEF/ELF4 binds to the HDM2 promoter *in vivo*. FLAG-MEF/ELF4-bound DNA from 293T cells was immunoprecipitated with FLAG antibody or normal mouse IgG. RQ-PCR amplification was performed on the corresponding templates by using primers for HDM2. *B*, structure of the HDM2 promoter region (−82 to −122) (*schematic*). *C*, 293T cells were transfected with HDM2 promoter-driven luciferase reporter plasmid encoding wild-type (*B* (*a*)) or mutant (*B* (*b*)) protein. Luciferase activity by pcDNA alone was assigned a value of 1.0. The analysis was performed in triplicate assays, and the results were reproducible. The results are shown as the mean ± S.D. (*error bars*). *D*, 293T cells were co-transfected with pFLAG/MEF/ELF4 and pcDNA/Wt-NPM1 or pcDNA/Mt-A-NPM1. RQ-PCR amplification was undertaken on corresponding templates using primers for HDM2. The analysis was performed in triplicate assays, and the results were reproducible. The results are shown as the mean ± S.D. *, $p < 0.05$.

TABLE 1
Clinical and laboratory characteristics of patients (ranges shown in parentheses)

	Wt-NPM1	Mt-NPM1	*p*
No. of patients	14	8	
Sex			
Male	5	5	
Female	9	3	0.60
Median age (years)	54.5 (18–78)	62 (44–76)	
FAB classification			
M0	1	0	
M1	2	2	
M2	4	2	
M4	2	2	
M5	2	2	
M6	3	0	0.50
TLD^+	6	4	0.50
Median white blood cell count/μl	7300 (1300–556,000)	47,500 (1700–114,700)	0.10
Median lactate dehydrogenase level	647 (203–5325)	669 (270–2391)	0.07
Median bone marrow cell count/μl	337,000 (9000–738,000)	475,000 (34,900–769,000)	0.10

levels of MEF/ELF4 (the MEF/ELF4-L group) ($p = 0.03$) (Fig. 8*B*).

DISCUSSION

In the present study, we identified NPM1 to be a MEF/ELF4-binding protein. Wt-NPM1 inhibited the function of MEF/ELF4 (*i.e.* DNA binding and transcriptional activities), whereas Mt-NPM1 augmented its function. Some of these effects of Wt-NPM1 and Mt-NPM1 on MEF/ELF4 were reproducible on the HDM2 promoter (one of the target genes of MEF/ELF4), suggesting that HDM2 expression is influenced by NPM1. Furthermore, we found that the expression of Mt-NPM1 in MEF/ELF4-overexpressing NIH3T3 cells resulted in enhanced malignant transformation. We also found that the mRNA level of *HDM2* in primary leukemia cells was higher in patients with NPM1 mutations. Mef/Elf4 directly activates *Mdm2* expression (13). Therefore, NPM1 mutation could enhance HDM2 expression through the increased MEF/ELF4 activity, thereby promoting transformation by inhibiting the p53 pathway.

NPM1 is a multifunctional phosphoprotein that has been implicated in cell proliferation as well as regulation of transcription factors. It appears to repress or stimulate transcription. For example, Wt-NPM1 activates and inhibits p53 function through direct binding (22, 25). Interferon regulatory factor-1 (IRF-1), a transcriptional activator, binds to Wt-NPM1, resulting in the inhibition of DNA binding and transcriptional activity (26). Our findings with Wt-NPM1 and MEF/ELF4 are consistent with these observations. Wt-NPM1 interacts directly with c-Myc and regulates the expression of

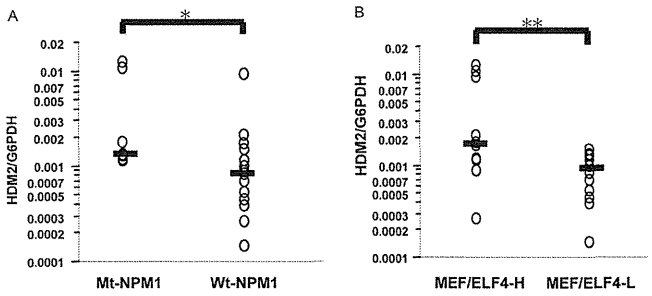

FIGURE 8. **Expression of Mt-NPM1 and higher expression of MEF/ELF4 are associated with the elevated expression of HDM2 in CD34-positive AML cells.** Total RNA isolated from 22 AML patients (CD34-positive leukemia cells) was analyzed for the expression of HDM2 by RQ-PCR. Shown is stratification by the presence of the NPM1 mutation (*A*) and by the level of ELF4/MEF (*B*). These bars were median lines for each group. *, $p < 0.009$ against Wt-NPM1; **, $p < 0.03$ against MEF/ELF4-L, assessed by analysis of variance followed by Scheffe's multiple comparison test.

endogenous c-Myc target genes at the promoter, which enhances c-Myc-induced proliferation and transformation (27). In contrast, the present study suggests that Wt-NPM1 inhibits (whereas Mt-NPM1 facilitates) the transformation induced by MEF/ELF4, suggesting that there is a contradiction in terms of NPM1 function. However, the overexpression of Wt-NPM1 without c-Myc activation has only a small effect on proliferation and has no effect on transformation, so Wt-NPM1 may mainly have a role in c-Myc-driven tumors. Interestingly, c-Myc, IRF-1, and MEF/ELF4 are all regulated during the cell cycle, and the levels of these transcription factors are highest in the G_1 phase (28, 29).

We found that Wt-NPM1 could interfere with the ability of MEF/ELF4 to bind to DNA, resulting in the inhibition of MEF/ELF4-dependent transcriptional activity. The mechanism by which Wt-NPM1 interferes with the DNA binding of MEF/ELF4 is unclear. We previously showed that the 120 amino acids N-terminal to the ETS domain in MEF/ELF4 (residues 87–206) are responsible for its binding to AML1 proteins (30); thus, MEF/ELF4 interacts with other proteins outside the DNA-binding domain. As mentioned above, the association of Wt-NPM1 and IRF-1 inhibits the DNA binding of IRF-1. Narayan *et al.* showed that IRF1 binds directly to Wt-NPM1 through a short linear motif in the nuclear localization sequence outside the DNA-binding domain (31). These results suggest that the inhibition of DNA binding by NPM1 may not be through simple interference with the DNA-binding domain of MEF/ELF4. Determining the protein-binding interface of MEF/ELF4 may help to reveal the mechanism of NPM1-mediated transcriptional regulation.

The heterodimerization domain (residues 186–259) of NPM1 is essential for its interaction with p53 (22), and the c-Myc-binding region is within the NPM1 heterodimerization domain (27). In the case of MEF/ELF4 and NPM1, the N-terminal regions of NPM1 (F1, F2, and F3) could bind to His-MEF/ELF4, implying that the oligomerization domain is important for the interaction.

Recently, it has been shown *in vivo* that NPM1 mutants actively contribute to leukemogenesis by conferring a proliferative advantage in the myeloid lineage. In zebrafish, forced expression of mutant NPM1 causes an increase in PU.1-positive primitive early myeloid cells (32). Furthermore, in a transgenic mouse expressing the human NPM1 mutant, although spontaneous AML was not found, myeloproliferation occurred in the bone marrow and spleen (33). Moreover, Vassiliou *et al.* (34) showed that activation of a humanized mouse NPM1 mutant knock-in allele in mouse hematopoietic stem cells caused overexpression of the *Hox* gene, enhanced self-renewal, and expanded myelopoiesis, resulting in delayed onset AML in one-third of the mice. Taken together, these data suggest that NPM1 mutations initiate leukemia by activating a set of proliferative pathways. Mt-NPM1 enhances the transcriptional activity of MEF/ELF4, so the up-regulation of HDM2 and subsequent down-regulation of p53 may also have a role in leukemogenesis.

In vitro transfection studies and immunohistochemical observations in samples from AML patients have demonstrated that NPM1 mutants recruit Wt-NPM1 from the nucleolus and delocalize it to the nucleoplasm and cytoplasm (18) and that aberrant NPM1 accumulation in the cytoplasm may have a critical role in leukemogenesis. While Wt-NPM1 protein co-localizes with tumor suppressor p19ARF in the nucleolus, Mt-NPM1 delocalizes p19ARF from the nucleolus to the cytoplasm, which results in reduced p19ARF activities (*e.g.* Mdm2 and $p21^{cip1}$ induction, stimulation of NPM1) (35). Furthermore, by using OCI/AML3 human leukemia cells where mutant NPM1 is localized in the cytoplasm, Bhat *et al.* (36) have recently shown that NPM1-co-localizing nuclear transcription factor, FOXM1 (forkhead box M1), disappears from the cytoplasm following transient NPM1 knockdown. These data suggest that NPM1 may determine the intracellular localization of interacting transcription factors. However, in our experiments, Mt-NPM1 did not interact with MEF/ELF4 *in vivo*, and the subcellular distribution of MEF/ELF4 was not affected by the presence of Mt-NPM1. It seems that Mt-NPM1 binds and dislocates Wt-NPM1 into the cytoplasm of leukemia cells, which eventually leads to uncontrolled transactivation of MEF/ELF4. Wt-NPM1 knockdown with siRNA against NPM1 also enhanced MEF/ELF4 activity (Fig. 3*E*), suggesting that the depletion of an MEF/ELF4 inhibitor (*i.e.* Wt-NPM1) in the nucleus is responsible for the transactivation of MEF/ELF4. Taken together, it is likely that NPM1 mutants exert oncogenic functions at least in part through the up-regulation of the activities of oncogenic transcription factors, such as MEF/ELF4. The correlation between NPM1 mutations and the elevated expression of HDM2 in primary leukemia cells seems to support this theory.

In patients with AML, NPM1 mutations are mutually exclusive of recurrent genetic abnormalities. It can be speculated that the enhanced MEF/ELF4-HDM2-p53 pathway induced by NPM1 mutations may participate in leukemia development, especially in patients with a normal karyotype. The transactivation of MEF/ELF4 by E2F1 is inhibited by p53 (37), suggesting that p53 suppression induced by NPM1 mutation could lead to the activation of E2F1, resulting in the enhanced expression of MEF/ELF4. Our previous data showing the elevated expression of MEF/ELF4 in AML cells with a normal karyotype compared with that of AML cells carrying t(8;21) and t(15;17) seem to support this hypothesis.

Our results suggest a new role for NPM1 and MEF/ELF4 in leukemia development.

REFERENCES

1. Miyazaki, Y., Sun, X., Uchida, H., Zhang, J., and Nimer, S. (1996) A novel transcription factor with an Elf-1 like DNA binding domain but distinct transcriptional activating properties. *Oncogene* **13,** 1721–1729
2. Hedvat, C. V., Yao, J., Sokolic, R. A., and Nimer, S. D. (2004) Myeloid ELF1-like factor is a potent activator of interleukin-8 expression in hematopoietic cells. *J. Biol. Chem.* **279,** 6395–6400
3. Lacorazza, H. D., Miyazaki, Y., Di Cristofano, A., Deblasio, A., Hedvat, C., Zhang, J., Cordon-Cardo, C., Mao, S., Pandolfi, P. P., and Nimer, S. D. (2002) The ETS protein MEF plays a critical role in perforin gene expression and the development of natural killer and NK-T cells. *Immunity* **17,** 437–449
4. Lu, Z., Kim, K. A., Suico, M. A., Shuto, T., Li, J. D., and Kai, H. (2004) MEF up-regulates human β-defensin 2 expression in epithelial cells. *FEBS Lett.* **561,** 117–121
5. Seki, Y., Suico, M. A., Uto, A., Hisatsune, A., Shuto, T., Isohama, Y., and Kai, H. (2002) The ETS transcription factor MEF is a candidate tumor suppressor gene on the X chromosome. *Cancer Res.* **62,** 6579–6586
6. Smith, A. M., Calero-Nieto, F. J., Schütte, J., Kinston, S., Timms, R. T., Wilson, N. K., Hannah, R. L., Landry, J. R., Göttgens, B. (2012) Integration of Elf-4 into stem/progenitor and erythroid regulatory networks through locus-wide chromatin studies coupled with *in vivo* functional validation. *Mol. Cell Biol.* **32,** 763–773
7. Lacorazza, H. D., Yamada, T., Liu, Y., Miyata, Y., Sivina, M., Nunes, J., and Nimer, S. D. (2006) The transcription factor MEF/ELF4 regulates the quiescence of primitive hematopoietic cells. *Cancer Cell* **9,** 175–187
8. Liu, Y., Elf, S. E., Miyata, Y., Sashida, G., Liu, Y., Huang, G., Di Giandomenico, S., Lee, J. M., Deblasio, A., Menendez, S., Antipin, J., Reva, B., Koff, A., and Nimer, S. D. (2009) p53 regulates hematopoietic stem cell quiescence. *Cell Stem Cell.* **4,** 37–48
9. Fukushima, T., Miyazaki, Y., Tsushima, H., Tsutsumi, C., Taguchi, J., Yoshida, S., Kuriyama, K., Scadden, D., Nimer, S., and Tomonaga, M. (2003) The level of MEF but not ELF-1 correlates with FAB subtype of acute myeloid leukemia and is low in good prognosis cases. *Leuk. Res.* **27,** 387–392
10. Yao, J. J., Liu, Y., Lacorazza, H. D., Soslow, R. A., Scandura, J. M., Nimer, S. D., and Hedvat, C. V. (2007) Tumor promoting properties of the ETS protein MEF in ovarian cancer. *Oncogene* **26,** 4032–4037
11. Totoki, Y., Tatsuno, K., Yamamoto, S., Arai, Y., Hosoda, F., Ishikawa, S., Tsutsumi, S., Sonoda, K., Totsuka, H., Shirakihara, T., Sakamoto, H., Wang, L., Ojima, H., Shimada, K., Kosuge, T., Okusaka, T., Kato, K., Kusuda, J., Yoshida, T., Aburatani, H., and Shibata, T. (2011) High-resolution characterization of hepatocellular carcinoma genome. *Nat. Genet.* **43,** 464–469
12. Du, Y., Spence, S. E., Jenkins, N. A., and Copeland, N. G. (2005) Cooperating cancer-gene identification through oncogenic-retrovirus-induced insertional mutagenesis. *Blood* **106,** 2498–2505
13. Sashida, G., Liu, Y., Elf, S., Miyata, Y., Ohyashiki, K., Izumi, M., Menendez, S., and Nimer, S. D. (2009) ELF4/MEF activates MDM2 expression and blocks oncogene-induced p16 activation to promote transformation. *Mol. Cell Biol.* **29,** 3687–3699
14. Borer, R. A., Lehner, C. F., Eppenberger, H. M., and Nigg, E. A. (1989) Major nucleolar proteins shuttle between nucleus and cytoplasm. *Cell* **56,** 379–390
15. Falini, B., Mecucci, C., Tiacci, E., Alcalay, M., Rosati, R., Pasqualucci, L., La Starza, R., Diverio, D., Colombo, E., Santucci, A., Bigerna, B., Pacini, R., Pucciarini, A., Liso, A., Vignetti, M., Fazi, P., Meani, N., Pettirossi, V., Saglio, G., Mandelli, F., Lo-Coco, F., Pelicci, P. G., Martelli, M. F., and GIMEMA Acute Leukemia Working Party (2005) Cytoplasmic nucleophosmin in acute myelogenous leukemia with normal karyotype. *N. Engl. J. Med.* **352,** 254–266
16. Yu, Y., Maggi, L. B., Jr., Brady, S. N., Apicelli, A. J., Dai, M. S., Lu, H., and Weber, J. D. (2006) Nucleophosmin is essential for ribosomal protein L5 nuclear export. *Mol. Cell Biol.* **26,** 3798–3809
17. Mariano, A. R., Colombo, E., Luzi, L., Martinelli, P., Volorio, S., Bernard, L., Meani, N., Bergomas, R., Alcalay, M., and Pelicci, P. G. (2006) Cytoplasmic localization of NPM in myeloid leukemias is dictated by gain-of-function mutations that create a functional nuclear export signal. *Oncogene* **25,** 4376–4380
18. Falini, B., Bolli, N., Shan, J., Martelli, M. P., Liso, A., Pucciarini, A., Bigerna, B., Pasqualucci, L., Mannucci, R., Rosati, R., Gorello, P., Diverio, D., Roti, G., Tiacci, E., Cazzaniga, G., Biondi, A., Schnittger, S., Haferlach, T., Hiddemann, W., Martelli, M. F., Gu, W., Mecucci, C., and Nicoletti, I. (2006) Both carboxyl-terminus NES motif and mutated tryptophan(s) are crucial for aberrant nuclear export of nucleophosmin leukemic mutants in NPMc+ AML. *Blood* **107,** 4514–4523
19. Grisendi, S., Bernardi, R., Rossi, M., Cheng, K., Khandker, L., Manovae, K., and Pandolfi, P. P. (2005) Role of nucleophosmin in embryonic development and tumorigenesis. *Nature* **437,** 147–153
20. Rigaut, G., Shevchenko, A., Rutz, B., Wilm, M., Mann, M., and Séraphin, B. (1999) A generic protein purification method for protein complex characterization and proteome exploration. *Nat. Biotechnol.* **17,** 1030–1032
21. Suzuki, T., Kiyoi, H., Ozeki, K., Tomita, A., Yamaji, S., Suzuki, R., Kodera, Y., Miyawaki, S., Asou, N., Kuriyama, K., Yagasaki, F., Shimazaki, C., Akiyama, H., Nishimura, M., Motoji, T., Shinagawa, K., Takeshita, A., Ueda, R., Kinoshita, T., Emi, N., and Naoe, T. (2005) Clinical characteristics and prognostic implications of NPM1 mutations in acute myeloid leukemia. *Blood* **106,** 2854–2861
22. Colombo, E., Marine, J. C., Danovi, D., Falini, B., and Pelicci, P. G. (2002) Nucleophosmin regulates the stability and transcriptional activity of p53. *Nat. Cell Biol.* **4,** 529–533
23. Phelps, M., Darley, M., Primrose, J. N., and Blaydes, J. P. (2003) p53-independent activation of the hdm-P2 promoter through multiple transcription factor response elements results in elevated hdm2 expression in estrogen receptor α-positive breast cancer cells. *Cancer Res.* **63,** 2616–2623
24. Grisendi, S., Mecucci, C., Falini, B., and Pandolfi, P. P. (2006) Nucleophosmin and cancer. *Nat. Rev. Cancer* **6,** 493–505
25. Li, J., Zhang, X., Sejas, D. P., and Pang, Q. (2005) Negative regulation of p53 by nucleophosmin antagonizes stress-induced apoptosis in human normal and malignant hematopoietic cells. *Leuk. Res.* **29,** 1415–1423
26. Kondo, T., Minamino, N., Nagamura-Inoue, T., Matsumoto, M., Taniguchi, T., and Tanaka, N. (1997) Identification and characterization of nucleophosmin/B23/numatrin which binds the anti-oncogenic transcription factor IRF-1 and manifests oncogenic activity. *Oncogene* **15,** 1275–1281
27. Li, Z., Boone, D., and Hann, S. R. (2008) Nucleophosmin interacts directly with c-Myc and controls c-Myc-induced hyperproliferation and transformation. *Proc. Natl. Acad. Sci. U.S.A.* **105,** 18794–18799
28. Amati, B., Alevizopoulos, K., and Vlach, J. (1998) Myc and the cell cycle. *Front. Biosci.* **3,** d250–d268
29. Miyazaki, Y., Boccuni, P., Mao, S., Zhang, J., Erdjument-Bromage, H., Tempst, P., Kiyokawa, H., and Nimer, S. D. (2001) Cyclin A-dependent phosphorylation of the ETS-related protein, MEF, restricts its activity to the G_1 phase of the cell cycle. *J. Biol. Chem.* **276,** 40528–40536
30. Mao, S., Frank, R. C., Zhang, J., Miyazaki, Y., and Nimer, S. D. (1999) Functional and physical interactions between AML1 proteins and an ETS protein, MEF. Implications for the pathogenesis of t(8;21)-positive leukemias. *Mol. Cell Biol.* **19,** 3635–3644
31. Narayan, V., Halada, P., Hernychová, L., Chong, Y. P., Žáková, J., Hupp, T. R., Vojtesek, B., and Ball, K. L. (2011) A multi-protein binding interface in an intrinsically disordered region of the tumor suppressor protein interferon regulatory factor-1. *J. Biol. Chem.* **286,** 14291–14303
32. Bolli, N., Payne, E. M., Grabher, C., Lee, J. S., Johnston, A. B., Falini, B., Kanki, J. P., and Look, A. T. (2010) Expression of the cytoplasmic NPM1 mutant (NPMc+) causes the expansion of hematopoietic cells in zebrafish. *Blood* **115,** 3329–3340
33. Cheng, K., Sportoletti, P., Ito, K., Clohessy, J. G., Teruya-Feldstein, J., Kutok, J. L., Pandolfi, P. P. (2010) The cytoplasmic NPM mutant induces myeloproliferation in a transgenic mouse model. *Blood* **115,** 3341–3345
34. Vassiliou, G. S., Cooper, J. L., Rad, R., Li, J., Rice, S., Uren, A., Rad, L., Ellis, P., Andrews, R., Banerjee, R., Grove, C., Wang, W., Liu, P., Wright, P.,

Arends, M., and Bradley, A. (2011) Mutant nucleophosmin and cooperating pathways drive leukemia initiation and progression in mice. *Nat. Genet.* **43,** 470–475

35. den Besten, W., Kuo, M. L., Williams, R. T., and Sherr, C. J. (2005) Myeloid leukemia-associated nucleophosmin mutants perturb p53-dependent and independent activities of the Arf tumor suppressor protein. *Cell Cycle* **4,** 1593–1598
36. Bhat, U. G., Jagadeeswaran, R., Halasi, M., and Gartel, A. L. (2011) Nucleophosmin interacts with FOXM1 and modulates the level and localization of FOXM1 in human cancer cells. *J. Biol. Chem.* **286,** 41425–41433
37. Taura, M., Suico, M. A., Fukuda, R., Koga, T., Shuto, T., Sato, T., Morino-Koga, S., Okada, S., and Kai, H. (2011) MEF/ELF4 transactivation by E2F1 is inhibited by p53. *Nucleic Acids Res.* **39,** 76–88

RADIATION RESEARCH 179, 361–382 (2013)
0033-7587/13 $15.00

DOI: 10.1667/RR2892.1

The Incidence of Leukemia, Lymphoma and Multiple Myeloma among Atomic Bomb Survivors: 1950–2001

Wan-Ling Hsu,[a] Dale L. Preston,[b,1] Midori Soda,[a] Hiromi Sugiyama,[a] Sachiyo Funamoto,[a] Kazunori Kodama,[a] Akiro Kimura,[c] Nanao Kamada,[d] Hiroo Dohy,[e] Masao Tomonaga,[f] Masako Iwanaga,[g] Yasushi Miyazaki,[h] Harry M. Cullings,[a] Akihiko Suyama,[a] Kotaro Ozasa,[a] Roy E. Shore[a] and Kiyohiko Mabuchi[i]

[a] *Radiation Effects Research Foundation, Hiroshima and Nagasaki, Japan;* [b] *Hirosoft International, Eureka, California;* [c] *Department of Hematology and Oncology, Hiroshima University, Hiroshima, Japan;* [d] *Hiroshima A-bomb Survivors Relief Foundation, Hiroshima, Japan;* [e] *Hiroshima Red Cross Hospital and Atomic-Bomb Survivors Hospital, Hiroshima, Japan;* [f] *The Japanese Red Cross Nagasaki Genbaku Hospital, Nagasaki, Japan;* [g] *Graduate School of Public Health, Teikyo University, Tokyo, Japan;* [h] *Department of Hematology, Nagasaki University, Nagasaki, Japan; and* [i] *Division of Cancer Epidemiology and Genetics, National Cancer Institute, Bethesda, Maryland*

Hsu, W. L., Preston, D. L., Soda, M., Sugiyama, H., Funamoto, S., Kodama, K., Kimura, A., Kamada, N., Dohy, H., Tomonaga, M., Iwanaga, M., Miyazaki, Y., Cullings, H., Suyama, A., Ozasa, K., Shore, R. and Mabuchi, K. The Incidence of Leukemia, Lymphoma and Multiple Myeloma among Atomic Bomb Survivors: 1950–2001. *Radiat. Res.* 179, 361–382 (2013).

A marked increase in leukemia risks was the first and most striking late effect of radiation exposure seen among the Hiroshima and Nagasaki atomic bomb survivors. This article presents analyses of radiation effects on leukemia, lymphoma and multiple myeloma incidence in the Life Span Study cohort of atomic bomb survivors updated 14 years since the last comprehensive report on these malignancies. These analyses make use of tumor- and leukemia-registry based incidence data on 113,011 cohort members with 3.6 million person-years of follow-up from late 1950 through the end of 2001. In addition to a detailed analysis of the excess risk for all leukemias other than chronic lymphocytic leukemia or adult T-cell leukemia (neither of which appear to be radiation-related), we present results for the major hematopoietic malignancy types: acute lymphoblastic leukemia, chronic lymphocytic leukemia, acute myeloid leukemia, chronic myeloid leukemia, adult T-cell leukemia, Hodgkin and non-Hodgkin lymphoma and multiple myeloma. Poisson regression methods were used to characterize the shape of the radiation dose-response relationship and, to the extent the data allowed, to investigate variation in the excess risks with gender, attained age, exposure age and time since exposure. In contrast to the previous report that focused on describing excess absolute rates, we considered both excess absolute rate (EAR) and excess relative risk (ERR) models and found that ERR models can often provide equivalent and sometimes more parsimonious descriptions of the excess risk than EAR models. The leukemia results indicated that there was a nonlinear dose response for leukemias other than chronic lymphocytic leukemia or adult T-cell leukemia, which varied markedly with time and age at exposure, with much of the evidence for this nonlinearity arising from the acute myeloid leukemia risks. Although the leukemia excess risks generally declined with attained age or time since exposure, there was evidence that the radiation-associated excess leukemia risks, especially for acute myeloid leukemia, had persisted throughout the follow-up period out to 55 years after the bombings. As in earlier analyses, there was a weak suggestion of a radiation dose response for non-Hodgkin lymphoma among men, with no indication of such an effect among women. There was no evidence of radiation-associated excess risks for either Hodgkin lymphoma or multiple myeloma. © 2013 by Radiation Research Society

INTRODUCTION

A radiation-related excess of leukemia in radiologists and physicians was recognized in the early 1940s (*1*, *2*). By the late 1940s, physicians in Hiroshima and Nagasaki had noticed an apparent increase in leukemia incidence among survivors (particularly children) who were near the hypocenters at the time of the atomic bombs. The first published report of an increased risk of leukemia among the atomic bomb survivors appeared in 1952 (*3*). Since then, risks of leukemia and other hematological malignancies have been the subject of special and continuing interest in studies of the survivors conducted at the Radiation Effects Research Foundation (RERF), formerly the Atomic Bomb Casualty Commission (ABCC).

The latest comprehensive analysis of the incidence of hematological malignancies in the RERF Life Span Study (LSS) cohort of the atomic bomb survivors (*4*) considered radiation effects on all leukemias as a group and on selected leukemia subtypes for the period from 1950–1987. Radiation effects on leukemia mortality have been considered in most of the periodic LSS mortality reports and

Note. The online version of this article (DOI: 10.1667/RR2892.1) contains supplementary information that is available to all authorized users.

[1]Address for correspondence: Department of Statistics, Radiation Effects Research Foundation, 5-2 Hijiyama Koen, Minami-Ku, Hiroshima 732-0815, Japan; e-mail: preston@hirosoft.net.

reports on dosimetry changes and temporal patterns of risk (*5–7*).

Incident cases used in the analyses presented here were identified by the Leukemia and Tumor/Tissue Registries in Hiroshima and Nagasaki with follow-up through the end of 2001, fifty-five years after the bombings and 14 years beyond that used in the previous comprehensive report. Analyses are presented for all leukemias other than chronic lymphocytic leukemia (CLL) or adult T-cell leukemia (ATL) as a group (leukemia other than CLL or ATL) as well as for major leukemia subtypes [acute myeloid leukemia (AML), acute lymphoblastic leukemia (ALL), chronic myeloid leukemia (CML)] and CLL, ATL, non-Hodgkin lymphoma (NHL), Hodgkin lymphoma (HL) and multiple myeloma (MM). In the leukemia analyses herein, we focus on how the excess risk varies with gender, age at exposure and attained age or time since exposure, as well as the characterization of curvature in the leukemia dose response. In contrast to the previous incidence analyses that focused solely on excess absolute rates (*4*), the present analyses focused on both excess relative risks and excess rates. A question of particular interest with regard to leukemia was whether or not there were any indications of a radiation-associated increase in risks 30 or more years after exposure. For lymphomas and MM, where the excess risks, if any, appear to be considerably lower than those for leukemia, our analyses primarily focused on the evidence for a statistically significant dose response.

MATERIAL AND METHODS

Study Population and Cohort Follow-up

In the late 1950s, records from the 1950 special national census of atomic bomb survivors were used by ABCC researchers to establish a fixed cohort of atomic bomb survivors: the LSS cohort. The LSS cohort includes 93,741 survivors who were residents of Hiroshima and Nagasaki, were present within 10 km of the hypocenters at the time of the bombs and were alive on October 1, 1950, and 26,580 Hiroshima and Nagasaki residents who were not in the cities at the time of the bombings. The latter group, which is referred to as the not-in-city (NIC) group, is similar in size and frequency-matched on gender and age at the time of the bombings to survivors in the cohort who were within 2.5 km of the hypocenters. The present analyses were based on the 113,011 cohort members for whom dose estimates are available. Dose estimates are not available for 7,044 cohort members because of uncertain locations or shielding configurations. Almost 60% of the cohort members are women and 41% were less than 20 years old at the time of the bombings. As of the end of follow-up for the present analyses (December 31, 2001), 43% of the cohort members were still alive. Additional information on the characteristics and history of the LSS cohort can be found in previously published articles (*4–6, 8*).

Until recently, it has been customary to exclude the NIC group from risk analyses because concerns about possible differences in socioeconomic status or other factors that might affect risk estimates. However, as in the most recent LSS solid cancer incidence analyses (*9*), the NIC group was used in this work to augment the information on variation in baseline rates by gender, attained age and birth cohort, but not on the overall level of the rates. This was accomplished by the inclusion of fitted increments associated with a city-specific NIC indicator in the baseline risk model.

Vital status for individual LSS cohort members is ascertained by linkage to the national family registration (*koseki*) system on a 3-year cycle. Given the comprehensive nature of the *koseki* system, only 175 (<1%) cohort members have been lost to follow-up. Information from *koseki* records is used to trace death certificates, which provide information on causes of death for those known to have died. Incidence follow-up began on October 1, 1950. The end of follow-up is the earliest date of diagnosis of the first primary malignancy (of any type), the date of death, the date of loss to follow-up or December 31, 2001.

Ascertainment of Hematological Malignancies

Leukemia registry. Two to three years after the atomic bombings of Hiroshima and Nagasaki, a number of physicians in Hiroshima and Nagasaki noted a markedly increased rate of leukemia in children living near the hypocenters (*3*). Therefore, in the early 1950s, ABCC researchers together with hematologists in Hiroshima and Nagasaki launched the Leukemia Registry program to ascertain all potential cases of leukemia and other hematological malignancies in the two areas, including cases that occurred in the late 1940s. The Leukemia Registry remained active until the late 1980s when it was supplanted by the city and prefecture cancer registries. Leukemia Registry data were the basis for a number of reports on radiation-related risk of leukemia and related diseases in the survivors (*10–15*).

The Leukemia Registry also gathered blood smears or other biological specimens used for diagnosis, clinical information, laboratory records and other material relevant to the diagnosis. These materials and information stored at ABCC and later at RERF were reviewed by at least two Leukemia Registry hematologists to develop a consensus diagnosis. Additional information on the Leukemia Registry procedures is available elsewhere (*4, 16*). Accepted cases were assigned a diagnosis date and the type of malignancy was coded. In the mid-1980s, the materials collected by the Leukemia Registry were re-reviewed and 60% of the leukemia diagnoses were classified using the French-American-British (FAB) classification system (*17–20*).

Tumor registries. As the Leukemia Registry activities declined in the mid-1980s, the population-based Tumor Registries, independent of the Leukemia Registry, became the primary source for ascertaining leukemias and other hematological malignancies in Hiroshima and Nagasaki. The Tumor Registries were established in 1957 in Hiroshima and 1958 in Nagasaki (*21*). The Hiroshima and Nagasaki Tumor Registries are operated by RERF entrusted by Hiroshima and Nagasaki prefectures and cities. Active ascertainment from hospital records in the two cities and their outlying areas is the primary method of case identification employed by the registries. Furthermore, this is supplemented by linkage to the cause of death information and to records from the ABCC surgical pathology program, which was superseded in the early 1970s by the regional tissue registries. Records are reviewed by RERF personnel trained in nosology and coded using the International Classification of Diseases for Oncology (ICD-O) codes that were current at the time of coding (*22*).

Assembling the present case series. Incident cases considered for these analyses were ascertained and assembled from the Leukemia Registry and the Hiroshima and Nagasaki Tumor Registries using a series of rules to give precedence to the better information when there were discrepancies. Since the Leukemia Registry involved detailed hematology review, precedence was given to the Leukemia Registry diagnosis if it was at least as detailed as the Tumor Registry diagnosis. Additional review was carried out for a small number of cases in which the Leukemia Registry and Tumor Registry diagnoses appeared to be inconsistent. More detailed information can be found in (*4*).

Classification of hematologic malignancies has been modified and refined over time, particularly for myeloid leukemias. Since most of the cases in these analyses cannot be classified according to the more detailed modern classifications and the number of cases of specific

subtypes tends to be small, we used a broad classification of types for these analyses that parallels the classification used in earlier reports on risks for these cancers in the LSS. In particular, cases identified as aleukemic/subleukemic myeloid leukemias and myeloid leukemia not otherwise specified are included in the AML group. The aleukemic/subleukemic lymphoid leukemias are combined with ALL. The CLL group includes CLL and hairy cell leukemia. ICD-O morphology codes included in the various analysis groups are given in supplementary Table S1 (http://dx.doi.org/10.1667/RR2892.1.S1)

Organization of the data for analysis. The primary Poisson regression analyses for this report were based on a highly stratified tabulation of person-years and case counts. The stratifying factors were: city, gender, age at exposure (5-year categories to age 69 and 70 and over), attained age (5-year categories from age 5–84 and 85 and over), calendar time period (from October 1, 1950, with subsequent cut points on January 1 of 1953, 1956 and 1958, and every 5 years from 1961–2001 except for an additional cut-point at 1988 to facilitate comparison with the previous report), exposure status (<3 km from the hypocenter, 3–10 km from the hypocenter and not in a city), adjusted and truncated weighted (gamma plus 10 times the neutron) bone marrow dose (22 dose categories for survivors), and whether or not an individual's shielded kerma estimate was greater than 4 Gy based on the latest dosimetry system (DS02). The lowest dose category included people whose DS02 weighted bone marrow dose estimates were less than 5 mGy. The lower dose bounds (in Gy) for the subsequent categories were: 0.005, 0.02, 0.04, 0.06, 0.08, 0.10, 0.125, 0.150, 0.175, 0.20, 0.25, 0.30, 0.50, 0.75, 1.0, 1.25, 1.5, 1.75, 2.0, 2.5, and 3.0. As in other LSS incidence reports (*4*, *9*), person-years were adjusted by birth cohort, time period, gender and city-specific residence probabilities to correct for migration from the Tumor Registries' catchment areas (*23*). A table with information on the proportion of person-years lost due to migration is given in supplementary Table S3 (http://dx.doi.org/10.1667/RR2892.1.S2). The data for each stratum included migration-adjusted person-years, counts of the number of eligible cases by outcome type, and person-year-weighted mean values of weighted bone marrow dose, attained age, age at exposure and time since exposure.

Risk Models and Statistical Methods

The previous analyses (*4*) focused on age at exposure dependent excess absolute rate (EAR) models in which the radiation dose effect could vary with time since exposure within age at exposure groups. As we examined the current data, it became apparent that simpler models similar to those used for solid cancers (*9*), in which the excess risk varies smoothly with age at exposure and time can often describe the data at least as well as the models used in the previous analyses. Therefore, we considered both EAR and excess relative risk (ERR) models in which the excess risk varies with age at exposure and either attained age or time since exposure. In an EAR model, the disease rate can be written as:

$$\lambda_0(c,s,a,b) + \rho(d)\varepsilon_a(c,s,a,b).$$

While in the ERR model it is

$$\lambda_0(c,s,a,b)[1 + \rho(d)\varepsilon_r(c,s,t,e)].$$

The term $\lambda_0(c,s,a,b)$ is a parametric model for the baseline (zero dose) rates that depends on attained age (a), gender (s), and factors such as birth cohort (b) and city (c). In the primary dose-response model, $\rho(d)\varepsilon(c,s,t,e)$, $\rho(d)$ describes the shape of the dose response and $\varepsilon(c,s,t,e)$ describes effect modification associated with the effect of dose d, i.e., how the level of the radiation-related excess risk varies with city (c), gender (s), age at exposure (e) and time (t), where time can be functions of either time since exposure or attained age. For this report (as in most analyses of the LSS data) effect modification was described using log-linear functions of the variables of interest. In descriptions of these models, unless explicitly noted, they are based on log attained age and log time since exposure. In general, age at exposure and time since exposure were centered or scaled so that the dose-effect parameters correspond to the risk for a person who was 30 years old at the time of the bombings for incidence 25 (attained age 55) or 40 (attained age 70) years after exposure. For some outcomes, we considered extensions of the effect modification model, including gender-dependent age at exposure and time effects, interactions between age at exposure and time, or categorical age at exposure and time effects.

The dose response functions considered in this report included:

(a) linear $\rho(d) = \beta_1 d;$

(b) linear – quadratic $\rho(d) = \beta_1 d + \beta_2 d^2;$

(c) pure – quadratic $\rho(d) = \beta_2 d^2;$

(d) single knot linear spline/threshold models

$$\rho(d) = \theta_1 d + \theta_2 (d - c)(d>c);$$

(e) nonparametric $\rho(d) = \theta_{dcat}.$

β_1 and β_2 are the linear and quadratic dose-response parameters, respectively. In a linear-quadratic model, the curvature of the dose response is defined as the ratio of the quadratic and linear dose effects: i.e., β_2/β_1. In the single-knot linear-spline/threshold models, c is a dose join point and when θ_1 equals 0 this is a threshold model. In the nonparametric dose-response model the dose response varies by dose category without any smoothing ($\rho(d) = \theta_{dcat}$). Although the bone marrow dose estimates used in all of these analyses were adjusted to allow for the effects of dose uncertainty (*24*), dose-response models also included a multiplicative dichotomous factor for those with shielded kerma estimates in excess of 4 Gy to allow for dose uncertainties not captured by the standard adjustment methods or for high-dose effects such as cell killing.

Analyses were limited to first primary malignancies diagnosed during the follow-up period among cohort members with DS02 dose estimates. Cases that were diagnosed outside of Hiroshima or Nagasaki prefectures were excluded. Maximum likelihood estimates of the parameters in these models were computed using the data in the person-year (PY) table described above. P values and confidence intervals (CI) for model parameters were based on the profile likelihood function. Uncertainty in the various risk estimates were summarized using 95% confidence intervals. The models were fit using the Epicure risk regression software (*25*). Akaike information criteria (AIC) (*26*) values were used to aid in the comparison of nonnested models. The models used are described and estimates of some of the key parameters are given in the Results section. However, details of the parameterizations used and the parameter estimates for our preferred models are presented in supplementary Table S2 (http://dx.doi.org/10.1667/RR2892.1.S1).

RESULTS

A total of 1,215 hematological malignancies were identified among 113,011 LSS cohort members and 944 of these cases were eligible for inclusion in the analyses between 1950 and the end of 2001. Almost 40% of the eligible hematopoietic malignancies were diagnosed after the end of the follow-up (1987) used in the last comprehensive analyses of the LSS data (*4*). Table 1 provides a summary of the numbers of cases eligible for

TABLE 1
Eligible and Ineligible Cases by Exclusion Reason

Malignancy	Eligible	Ineligible				Total
		Not first primary	Nonresident[†]	Unknown dose	Before 10/1/1950	
Leukemia						
Leukemia other than CLL or ATL	312	28	31	36	9	416
Acute myeloid (AML)[‡]	176	20	13	18	2	229
Chronic myeloid (CML)	75	3	5	11	5	99
Acute lymphoblastic (ALL)[§]	43	4	9	4	2	62
Other	18	1	4	3	0	26
Chronic lymphocytic (CLL)[††]	12	4	0	0	0	16
Adult T-cell (ATL)	47	3	7	2	0	59
Any leukemia	371	35	38	38	9	491
Lymphoma and Myeloma						
Non-Hodgkin lymphoma (NHL)	402	34	33	27	5	501
Hodgkin lymphoma (HL)	35	1	4	1	1	42
Multiple myeloma (MM)	136	26	10	9	0	181
Total	944	96	85	75	15	1,215

[†] Residing outside of Hiroshima or Nagasaki prefectures at the time of diagnosis.
[‡] Includes acute myeloid leukemia (146 eligible cases) as well as acute monocytic leukemia (10 eligible cases), a-/sub-leukemic myeloid leukemia (16 eligible cases) and myeloid leukemia NOS (4 eligible cases).
[§] Includes 41 cases classified as acute lymphoblastic leukemia (41 cases) and 2 cases classified as aleukemia/subleukemic lymphoid leukemia.
[††] Includes 10 cases classified as chronic lymphocytic leukemia and 2 as hairy cell leukemia.

dose-response analyses by type of malignancy together with information on the reasons why cases were deemed ineligible. About 40% of the cases were leukemias, another 40% were identified as NHL and almost 15% were MM. Hodgkin lymphoma was uncommon. Almost half of the leukemia cases were classified as AML, 20% were CML and about 12% were ALL. All but five of 47 ATL cases were diagnosed in Nagasaki and constitute almost 40% of all of the Nagasaki leukemia cases. As with other populations in Japan, the incidence of CLL is remarkably low. All except 3 of 18 cases in the *other leukemia* group were diagnosed in Hiroshima. Eleven of the cases in this group were classified as acute leukemia not otherwise specified (NOS) and other specific types of leukemia while 7 were classified as aleukemia, subleukemia or leukemia NOS. The cases in this group were included in the leukemia other than the CLL or ATL analyses discussed below but were not analyzed separately. The crude rates for leukemia, lymphoma and multiple myeloma by age at exposure, period and dose category are given in supplementary Tables S4 and S5 (http://dx.doi.org/10.1667/RR2892.1.S2).

Leukemia Other Than CLL or ATL

While a few studies suggest that CLL risk may be affected by radiation exposure (*27–30*), a number of others do not (*31*, *32*). It is generally believed that radiation has little effect on CLL rates and it is common practice in studies of radiation effects to focus on the risk of leukemia other than CLL. In view of the unusual nature of ATL incidence, we also excluded ATL from the pooled leukemia analyses. A total of 312 cases of leukemia other than CLL or ATL were used in these analyses (Table 1).

Baseline rates for this outcome were described reasonably well by a model in which the rates increased in proportion to age. This simple pattern was significantly improved ($P < 0.001$) by allowing the power to increase with increasing attained age (i.e., by adding a quadratic term in log attained age). The nature of the increase with attained age did not differ significantly by gender ($P > 0.5$), nor did it appear to vary significantly with birth cohort ($P = 0.30$). However, at any given age the risk for women was about half that for men (female:male ratio 0.50 95% CI 0.40–0.63). Baseline rates in Nagasaki were 35% lower than in Hiroshima ($P = 0.004$). There was a significant ($P < 0.001$) nonlinear birth cohort effect with the highest age-specific rates for those born around 1920, which decreased by about 30% for people born 20 years earlier or later than this—a pattern similar to that seen in the Japanese national leukemia mortality rates (*33*). The fitted age-specific baseline rate estimates for three birth cohorts are shown in Fig. 1a. The baseline rate model and parameter estimates for leukemias other than CLL or ATL are given in supplementary Table S2 (http://dx.doi.org/10.1667/RR2892.1.S1).

Dose response and effect modification. Using a simple time-constant linear ERR model with no effect modification, there was a statistically significant ($P < 0.001$) dose-response relationship. Allowing for attained age and time since exposure effects (discussed below), a concave upward linear-quadratic (LQ) model described the data significantly better than either a linear dose response ($P = 0.001$) or pure-quadratic ($P = 0.04$) dose-response model. The estimated linear dose effect in the LQ ERR model at attained age 70 after exposure at age 30 was 0.79 per Gy and the estimated curvature was 1.20, as given in Table 3. Figure 1b illustrates the fitted dose response together with dose-category-

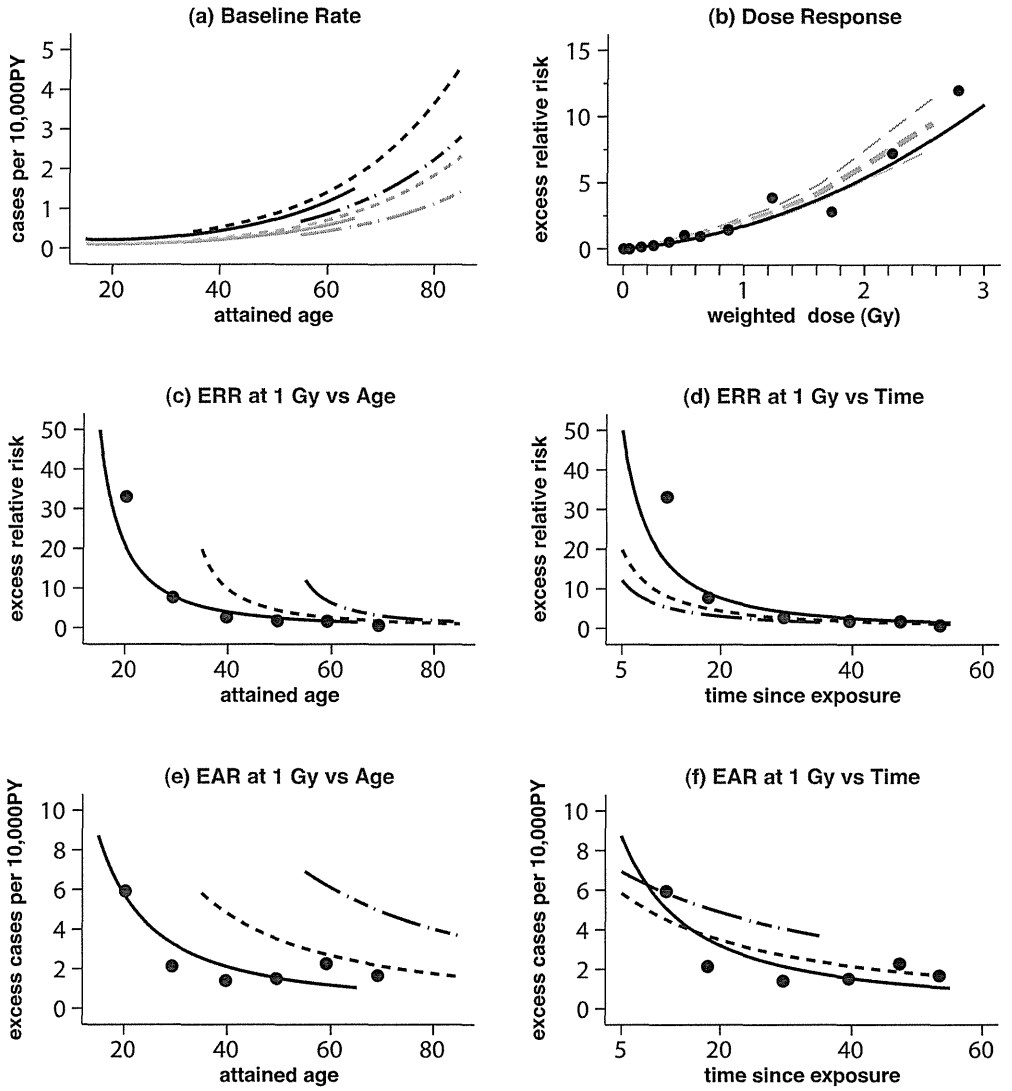

FIG. 1. Summaries of the risk of leukemia other than CLL or ATL in the LSS. Plot (panel a) shows age-specific baseline (zero dose) rates in Hiroshima for men (black lines) and women (gray lines) for LSS cohort members born in 1895 (dash-dot line; age at exposure 50), 1915 (dash line; age at exposure 30) and 1935 (solid line; age at exposure 10). Panel b: illustrates the radiation dose response based on the ERR model with risks standardized to attained age 70 for a person exposed at age 30 (born in 1915). The solid-black line illustrates the fitted linear-quadratic dose response. The points are based on a nonparametric dose-response model, while the middle-dashed-gray line is a smoothed version of the dose category-specific estimates from the nonparametric fit. The upper- and lower-dashed-gray line are plus and minus one standard error from the smoothed fit. Panels c and d: illustrate the temporal pattern and age-at-exposure effects for our preferred ERR model. The fitted ERR did not depend on either gender or city. Panels e and f: present the temporal pattern and age-at-exposure effects for Hiroshima males based on the preferred EAR model. The points in panels c–f are nonparametric estimates for exposure at age 10.

specific standardized ERR estimates and a dose-response function defined by smoothing the category-specific standardized estimates.

Based on our preferred ERR model (described below), it was estimated that about 94.1 of the 312 cases of leukemia other than CLL or ATL used in these analyses were associated with the radiation exposure (Table 2). The radiation-associated excess cases account for about 49% of the 192 cases among cohort members with doses in excess of 5 mGy.

Parameter estimates and confidence intervals for the preferred model for leukemia other than CLL or ATL are given in Table 3. The ERR was found to depend jointly on log attained age ($P < 0.001$) and either age at exposure ($P = 0.01$) or time since exposure ($P = 0.003$). These two models (age and age at exposure or age and time since exposure) led to similar patterns of the excess risk. However, since the fit of the age and time since exposure model (AIC = 2431.89) was somewhat better than that for the age and age at exposure model (AIC = 2433.97), our preferred model

TABLE 2
Observed and Fitted Cases of Leukemia Other than CLL or ATL by Weighted Bone Marrow Dose Categories

Dose (Gy)	Person years	Mean dose (Gy)	Observed cases	Fitted cases†	
				Background	Excess
<0.005	2,039,093	0.0006	120	116.9	0.1
–0.1	957,889	0.03	63	60.7	3.6
–0.2	201,935	0.14	16	13.7	4.1
–0.5	206,749	0.32	25	13.6	11.1
–1	117,855	0.71	24	7.5	18.2
–2	64,122	1.37	35	4.0	28.4
2+	25,761	2.68	29	1.5	28.6
Total	3,613,404	0.10	312	217.9	94.1

† Estimates based on the preferred ERR linear-quadratic model described in the text and Table 3 with additional details in supplementary Table S2 (http://dx.doi.org/10.1667/RR2892.1.S1).

includes age and time since exposure as effect modifiers. As indicated in the upper portion of Table 3, with both of these temporal factors in the model, the decrease in the ERR with increasing attained age was proportional to attained age to the power −1.09 and simultaneously proportional to time since exposure to the power −0.81. The model predicted that the highest ERRs were seen shortly after exposure among those exposed early in life (Fig. 1d). However, due to the rapid decline in the ERR with time, at any given attained age the ERR was greater for those who were exposed at older ages (Fig. 1c). There was no indication that the ERR varied significantly with gender ($P = 0.29$) or city ($P = 0.42$), nor did it appear that the dose-response curvature varied with city ($P > 0.5$). The precise form of this model is indicated in supplementary Table S2 (http://dx.doi.org/10.1667/RR2892.1.S1) and information on the fit of alternative models is given in supplementary Table S6 (http://dx.doi.org/10.1667/RR2892.1.S2).

The excess absolute rates for leukemia other than CLL or ATL could also be described by a linear-quadratic EAR model in which the radiation-associated excess rate depended on attained age ($P < 0.001$), age at exposure ($P < 0.001$) and city ($P = 0.03$), with a suggestion of a statistically significant gender difference ($P = 0.08$). This EAR model (AIC = 2433.2) describes the data slightly worse than the preferred ERR model discussed above. An EAR model with log-time since exposure and age-at-exposure effects (AIC = 2,438.8) fit worse than the preferred attained age and age-at-exposure model. Adding attained age to this time-since-exposure model led to a statistically significant improvement in fit ($P < 0.001$). The resulting model was virtually identical to the attained-age model. Thus, attained age with an age-at-exposure effect provided a better description of the temporal variation of EAR than did attained age with a time-since-exposure effect.

In our preferred EAR model (Table 3 and supplementary Table S6: http://dx.doi.org/10.1667/RR2892.1.S2), the linear dose coefficient estimates (standardized to age 70 after exposure at age 30) in Hiroshima were 1.06 excess cases per 10,000 PY per Gy for men and 0.7 for women with estimated curvature similar to the ERR model. The decrease

TABLE 3
Preferred Model, Excess Risk Parameter Estimates for Leukemia Other than CLL or ATL

Risk model	Dose coefficients (at 1 Gy)		Curvature	Gender ratio (F:M)	City ratio (N:H)	Attained age (power)	Time since exposure (power)	Age at exposure
	Linear	Quadratic						
ERR†	0.79	0.95	1.20			−1.09	−0.81	
	(0.03, 1.93)	(0.34, 1.80)	(0.23, 49.35)			(−2.01, −0.27)	(−1.31, −0.28)	
EAR‡								
Women	0.70	0.71	1.03	0.66	0.52	−1.45		0.41
	(0.13, 1.53)	(0.24, 1.41)	(0.20, 8.52)	(0.41, 1.04)	(0.26, 0.93)	(−2.13, −0.80)		(0.2, 0.64)
Men	1.06	1.09						
	(0.16, 2.42)	(0.37, 2.13)						

† The preferred ERR model is linear quadratic in dose with log-linear effect modification depending on log (attained age) and log (time since exposure). The baseline model parameters and explicit details about the dose effect modification term are given in supplementary Table S2 (http://dx.doi.org/10.1667/RR2892.1.S1). Supplementary Table S6 (http://dx.doi.org/10.1667/RR2892.1.S2) presents information on other ERR models. The dose coefficients describe the ERR at 1 Gy at age 70 after exposure at age 30.

‡ The preferred EAR model is linear-quadratic in dose with log-linear effect modification depending on log (attained age) and age at exposure. The baseline model parameters and explicit details about the dose effect modification term is given in supplementary Table S2 (http://dx.doi.org/10.1667/RR2892.1.S1). Supplementary Table S6 (http://dx.doi.org/10.1667/RR2892.1.S2) presents information on other EAR models. The dose coefficients describe the excess cases per 10,000 person years at 1 Gy at age 70 after exposure at age 30.

TABLE 4
Observed and Fitted Excess Cases of Leukemia Other than CLL or ATL by Time Period and Age at Exposure with Category-Specific ERR Estimates

	Age at exposure									
	0–19		20–39		40+		Total			
Period	Obs	Exc[†]	Obs	Exc	Obs	Exc	Obs	Exc	ERR[‡] (95%CI)	
1950–1955	18	16.2	11	6.5	13	7.6	42	30.3	15.2	(8.8 to 25)
1956–1959	17	5.4	4	4.1	18	4.7	39	14.2	13.3	(7.2 to 23)
1960–1969	14	6.3	17	6.5	19	6.0	50	18.8	4.8	(2.3 to 8.4)
1970–1979	11	4.7	33	5.3	18	3.2	62	13.2	3.4	(1.5 to 6.3)
1980–1989	17	4.4	25	4.3	12	1.3	54	9.9	1.8	(0.5 to 3.8)
1990–2001	29	4.3	32	3.0	4	0.3	65	7.6	2.1	(0.8 to 4.3)
Total	106	41.3	122	29.7	84	23.1	312	94.0		
ERR[‡] (95% CI)	6.5 (4.0 to 10.3)		3.9 (2.3 to 6.1)		4.0 (2.1 to 6.9)		4.7 (3.3 to 6.5)			

[†] Excess cases based on preferred ERR model described in the text and Table 3 with additional details in supplementary Table S2 (http://dx.doi.org/10.1667/RR2892.1.S1).

[‡] ERR at 1 Gy for a linear dose response model with categorical period or age at exposure effects.

in the EAR with attained age was proportional to age to the power −1.45, while the EARs for a given attained age were estimated to increase by about 51% per decade increase in age at exposure (95% CI 23–89%). Excess rates for Nagasaki survivors were estimated to be about 52% of those for Hiroshima survivors of the same gender and exposure age, and excess rate estimates for women were about 66% of those for men. The variation in the fitted EAR estimates with attained age and time since exposure for various ages at exposure are shown in Fig. 1e and f, respectively.

We used a simple ERR model with categorical main effects for six time periods and three age-at-exposure groups to examine whether or not the risks had persisted throughout the follow-up period. As indicated by the results summarized in Table 4, there was evidence of statistically significant increased risks in each of the six time periods considered. The largest ERRs were seen for the two earlier periods. However, even for the last 12 years of follow-up (1990–2001 or 45–55 years after exposure), the radiation-associated leukemia risk at 1 Gy was estimated to be twice the baseline risk.

Acute Myeloid Leukemia (AML)

There were 176 eligible AML cases, including 42 cases diagnosed after 1987 among LSS cohort members who were in the cities at the time of the bombings and 15 cases among cohort members who were NIC at the time of the bombings.

As indicated in Fig. 2a, AML baseline rates increased with attained age, but the level of risk and the nature of the increase with age differed for men and for women ($P < 0.001$). Baseline rates for women were about 40% (95% CI 29–56%) of those for men, and the rate of increase with attained age was more rapid for men than for women ($P = 0.04$). The baseline rates also exhibited a complex birth cohort effect. Age-specific rates were larger for people born between 1915 and 1925 than for people born before or after this period ($P < 0.001$). This pattern is similar to that seen in the Japanese national leukemia mortality rates, but somewhat more pronounced in the LSS cohort. The baseline AML rates in Nagasaki were 25% lower, though not significantly lower ($P = 0.14$), than those in Hiroshima. The AML baseline rate model and parameter estimates are given in supplementary Table S2 (http://dx.doi.org/10.1667/RR2892.1.S1).

Dose response and effect modification. There was strong evidence for a radiation dose-response relationship ($P < 0.001$). As shown in Fig. 2B, the dose-response curve was concave upward ($P = 0.01$). A pure-quadratic model with an estimated ERR at 1 Gy of 1.11 (95% CI 0.53–2.08, standardized to age 70 after exposure at age 30) as shown in Table 6 described the data as well as a linear-quadratic model ($P > 0.5$). Inference about effect modification in the ERR and EAR was based on a pure-quadratic model. In our preferred AML models (described below), the number of radiation-associated cases was estimated to be 37.4 (Table 5). The fraction attributable to radiation was 38% among cohort members with doses in excess of 5 mGy.

ERRs for AML exhibited a statistically significant [$P = 0.004$, with 2 degrees of freedom (*df*)] non-monotone dependence on age at exposure. As suggested in Fig. 2c, for any attained age (after exposure), the ERR for the people exposed around age 30 tended to be lower than for those exposed later or younger in life. The decrease in the ERR with attained age (AIC = 1,552.14) was well described as proportional to age to the power −0.89 (Table 6). More complex patterns for the age/time dependence were also considered. Neither the addition of a quadratic term in log age nor the use of splines in log age significantly improved the fit, nor did the use of functions of time since exposure result in better fits ($P > 0.5$ in every case). There was no indication of an attained age by age-at-exposure interaction ($P > 0.5$), nor did the attained age or age-at-exposure effects appear to vary with gender ($P > 0.5$). Parameter estimates with confidence intervals for the preferred AML,

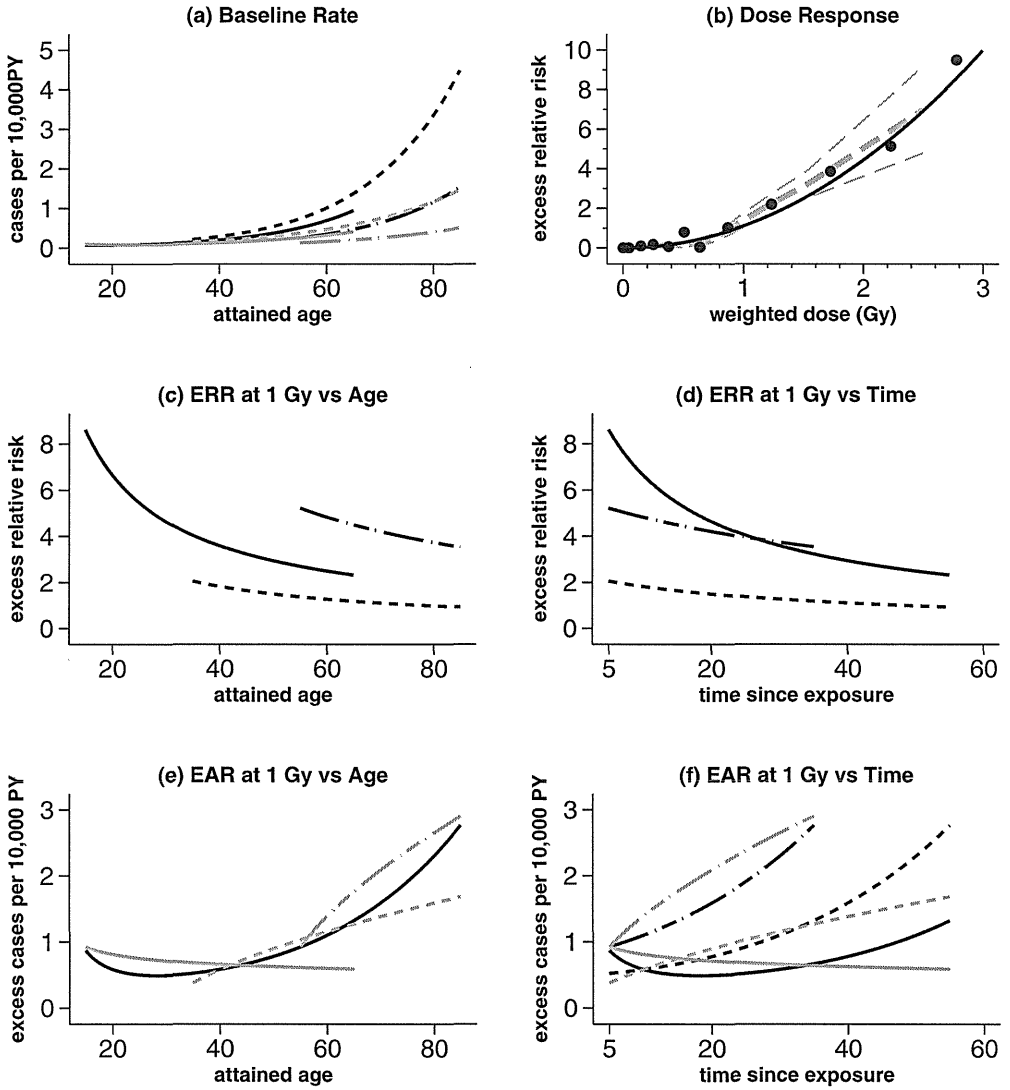

FIG. 2. LSS acute myeloid leukemia risk summary plots. Panel a: shows age-specific rates in the Hiroshima baseline (zero dose) for men (black lines) and women (gray lines) for LSS cohort members born in 1895 (dash-dot line; age at exposure 50), 1915 (dash line; age at exposure 30) and 1935 (solid line; age at exposure 10). Panel b: illustrates the radiation dose response based on the preferred ERR model with risks standardized to attained age 70 for a person exposed at age 30 (born in 1915). The solid-black line illustrates the fitted pure-quadratic dose response. The points are based on a nonparametric dose-response model, while the middle-dashed-gray line is a smoothed version of the dose category-specific estimates from the non-parametric fit. The upper- and lower-dashed-gray lines are plus and minus one standard error from the smoothed fit. Panels c and d: illustrate the temporal pattern and age-at-exposure effects for our preferred ERR model. Panels e and d: present the temporal pattern and age-at-exposure effects for Hiroshima males based on the preferred EAR model. Black lines are shown for ages at exposure of 10 (solid line), 30 (dash line) and 50 years (dash-dot line). The gray lines are the EAR temporal patterns using the model specified in a previous report (*4*). For the ERR and EAR models shown here, the excess risks did not depend on either gender or city.

ERR and EAR models are given in Table 6. Additionally, the precise form of this model is given in supplementary Table S2 (http://dx.doi.org/10.1667/RR2892.1.S1) and information on the fit of alternative models is given in supplementary Table S7 (http://dx.doi.org/10.1667/RR2892.1.S2).

The AML EAR was also described equally well (AIC = 1,550.0) using a model with a linear-quadratic effect in log attained age. This description of the temporal pattern of the AML, which is illustrated in Fig. 2e, is considerably simpler than the model used in the previous LSS leukemia incidence report (*4*). In that model, there were separate temporal patterns for each of three age-at-exposure groups, while all of the temporal variation excess rates in the current model are expressed in terms of age without the need for dependence on either age at exposure or time since exposure. Figure 2e and f shows the variation of the AML EAR with attained age and time since exposure based on the

TABLE 5
Observed and Fitted Background and Excess Cases of Acute Myeloid Leukemia by Weighted Bone Marrow Dose Category

Dose (Gy)	Person years	Observed cases	Fitted cases†	
			Background	Excess
<0.005	2,039,093	77	75.6	0.0
–0.1	957,889	36	37.7	0.2
–0.2	201,935	9	8.2	0.6
–0.5	206,749	12	8.4	2.7
–1	117,855	11	4.9	6.9
–2	64,122	18	2.8	14.0
2+	25,761	13	1.0	13.0
Total	3,613,404	176	138.6	37.4

† Estimates based on the preferred quadratic ERR model described in the text and Table 6 with additional details in supplementary Table S2 (http://dx.doi.org/10.1667/RR2892.1.S1).

current model together with using lighter lines, the pattern from an EAR model of the form used in the 1994 report. The new model predicts somewhat lower excess rates shortly after the bombings for those exposed as children, and somewhat higher rates throughout the follow-up for those exposed at age 50.

The fitted models illustrated in Fig. 2f reveal an upward trend in the AML excess rates in recent years, suggesting that excess risks have persisted throughout the entire follow-up period. Categorical analyses based on a simple model with main effects for three age-at-exposure and six period effects were used to assess the persistence of the risk. As seen in Table 7, there was evidence of increased risks in the last 12 years of follow-up with a significantly elevated ERR at 1 Gy of 1.5, representing about 6 excess cases during this period.

Acute Lymphoblastic Leukemia (ALL)

There were 43 eligible ALL cases. This relatively small number of cases, coupled with a large proportion (about half, described below) being associated with radiation exposure, makes it difficult to make precise inferences about the baseline rates. However, it appeared that ALL baseline rates increased with attained age ($P = 0.01$). This increase was estimated to be proportional to attained age to the power 1.70 (95% CI 0.34–3.36) (supplementary Table S2; http://dx.doi.org/10.1667/RR2892.1.S1), and allowing for more complex age patterns did not improve the fit. Population data for Japan and other countries (*34*) suggest that ALL baseline rates have a U-shaped pattern in which the rates reach a minimum in the 30–40 age range and increase at older ages. We did not find evidence for such a pattern in our data, most likely reflects the limited power due to the small number of cases in the cohort. There was no evidence of gender differences in either the level of risk ($P > 0.5$) or the age pattern ($P > 0.5$), nor were there any indications of a trend in the baseline rates with birth cohort ($P = 0.17$) or of city differences ($P = 0.43$). Figure 3a illustrates how the fitted baseline ALL rates vary with attained age. The ALL baseline rate model and parameter estimates are given in supplementary Table S2 (http://dx.doi.org/10.1667/RR2892.1.S1).

Dose response and effect modification. There was a significant linear dose-response relationship ($P < 0.001$) with some indication of upward curvature ($P = 0.05$), much of which was influenced by 4 cases with unweighted shielded kerma estimates in excess of 4 Gy. After adjusting for the high-dose cases by including a dichotomous indicator, there was no evidence of significant curvature ($P = 0.13$). Figure 3b shows the estimated linear dose response. In our preferred ALL model (described below), the number of radiation-associated ALL cases was estimated to be 21.6 (Table 8). About 67% of the cases among cohort members with doses in excess of 5 mGy were associated with radiation exposure.

The ERR for ALL decreased markedly over time ($P < 0.001$). This decrease was described as proportional to attained age to the power –3.51 (Table 9). The ERR for women was about 40% of that for men. This gender- and attained-age-dependent ERR model (AIC = 496.4) described the data better than a model that included joint effects of age at exposure (higher for younger ages) and time since exposure (decreasing with time) (AIC = 502.7). As illustrated in Fig. 3c, this model predicted extremely

TABLE 6
Preferred Model, Excess Risk Parameter Estimates for Acute Myeloid Leukemia

Risk model	Quadratic dose coefficient (at 1 Gy)	Attained age		Age at exposure	
		Linear	Quadratic	Linear	Quadratic
ERR†	1.11 (0.53, 2.08)	–0.89 (–2.29, 0.41)		0.17 (–0.15, 0.50)	0.25 (0.09, 0.41)
EAR‡	1.59 (0.95, 2.41)	2.59 (0.90,4.26)	1.43 (0.44, 2.32)		

† The preferred ERR model is quadratic in dose with log-linear effect modification depending on log(attained age) and a linear-quadratic function of age at exposure. The baseline model parameters and explicit details about the dose effect modification term are given in supplementary Table S2 (http://dx.doi.org/10.1667/RR2892.1.S1). Supplementary Table S7 (http://dx.doi.org/10.1667/RR2892.1.S2) presents information on alternative ERR models. The dose coefficients describe the ERR at 1 Gy at age 70 after exposure at age 30.

‡ The preferred EAR model is quadratic in dose with log-linear effect modification depending on a linear-quadratic function of log(attained age). The baseline model parameters and explicit details about the dose effect modification term is given in supplementary Table S2 (http://dx.doi.org/10.1667/RR2892.1.S1). Supplementary Table S7 (http://dx.doi.org/10.1667/RR2892.1.S2) presents information on alternative EAR models. The dose coefficients describe the excess cases per 10,000 person years at 1 Gy at age 70.

TABLE 7
Observed and Fitted Excess Cases of Acute Myeloid Leukemia by Time Period and Age at Exposure with Category-Specific ERR Estimates

	Age at exposure									
	0–19		20–39		40+		Total			
Period	Obs	Exc†	Obs	Exc	Obs	Exc	Obs	Exc	ERR‡	(95%CI)
1950–1955	4	3.1	3	0.7	4	2.5	11	6.4	3.6	(0.7 to 10.2)
1956–1959	7	1.3	3	0.7	8	2.2	18	4.2	9.0	(3.5 to 19.2)
1960–1969	7	2.1	7	1.7	10	3.9	24	7.7	3.1	(1.1 to 6.7)
1970–1979	7	2.3	21	2.1	13	2.4	41	6.8	1.9	(0.4 to 4.7)
1980–1989	12	3.0	20	2.2	7	1.1	39	6.3	1.8	(0.6 to 4.0)
1990–2001	19	3.9	23	1.9	1	0.3	43	6.1	1.5	(0.4 to 3.4)
Total	56	15.7	77	93	43	12.2	176	37.4		
ERR‡ (95% CI)	2.3 (1.0 to 4.5)		2.0 (0.9 to 3.8)		3.4 (1.5 to 6.6)		2.4 (1.5 to 3.7)			

† Excess cases based on preferred ERR model described in the text and Table 6 with additional details in supplementary Table S2 (http://dx.doi.org/10.1667/RR2892.1.S1).
‡ ERR at 1 Gy for a quadratic dose response model with categorical period and age-at-exposure effects.

large ERRs for those exposed as children. Virtually all of the 22 cases among those exposed before age 20 could be attributed to radiation exposure.

The radiation effect on the ALL risk could be described equally well (AIC = 496.4) using an EAR model, as illustrated in Fig. 3e. In our preferred EAR model, the excess rate decreased in proportion to age to the power −1.81 (Table 9). There was a significant gender difference ($P = 0.05$) with an estimated female:male EAR ratio of 0.40. The gender-averaged EAR at age 70 was 0.16 radiation-associated cases per 10,000 person years per Gy (95% CI 0.05– 0.38). Parameter estimates with confidence intervals for the preferred ALL ERR and EAR models are given in Table 9. The precise form of this model is given in supplementary Table S2 (http://dx.doi.org/10.1667/RR2892.1.S1) and information on the fit of alternative models is given in supplementary Table S8 (http://dx.doi.org/10.1667/RR2892.1.S2). The ALL EAR could be described almost as well using a combination of age-at-exposure and time-since-exposure effects in place of the attained age effect (supplementary Table S8; http://dx.doi.org/10.1667/RR2892.1.S2).

Both the ERR and EAR results indicated that the radiation-associated risks have decreased over time, but also suggested that dose-related increased risks may persist for many years after exposure. Using a simple ERR model in which the dose response was allowed to differ for the three periods of October 1950 through December 1952, 1953–1965 and 1966–2001, we found statistically significant dose-related increases in the risk for each period. Although the ERR decreased over time, the ERR for the last period was statistically significant and had a population average 3.1 (95% CI 0.6–10.4, $P = 0.001$) (results not shown).

Chronic Myeloid Leukemia (CML)

There were 75 eligible CML cases (63 in Hiroshima, 12 in Nagasaki) including 13 cases that occurred after 1987. The CML baseline rate increased with attained age ($P < 0.001$) with a significant difference in the age pattern for men and women ($P = 0.004$) (Fig 4a). Baseline rates for men were higher than those for women prior to age 75, but women had higher rates later in life, because the rates for women rose more rapidly than those for men. There was no indication of a birth cohort effect ($P > 0.5$). After allowing for a city difference in the dose response (described below), the baseline rates did not differ significantly by city ($P > 0.5$). The CML baseline rate model and parameter estimates are given in supplementary Table S2 (http://dx.doi.org/10.1667/RR2892.1.S1).

Dose response and effect modification. CML rates exhibited a statistically significant ($P < 0.001$) linear dose-response relationship that was not improved by the addition of a quadratic term ($P > 0.5$). The dose-response curve is shown in Fig. 4b. In our preferred ERR model for CML, the ERR was dependent on city and both time since exposure and attained age. As shown in Table 11, the estimated ERR was 5.24 per Gy standardized to attained age 55 and 25 years after exposure, and the ERR in Nagasaki was estimated to be 22% of that in Hiroshima ($P = 0.01$). There was no indication that the ERR differed by gender ($P > 0.5$).

The ERR decreased significantly in proportion to time since exposure to the power −1.59 at any attained age. The ERR decreased significantly in proportion to attained age to the power −1.42. Using the preferred ERR model the observed number of radiation-associated cases was estimated to be 33.4 with the attributable fraction among those exposed to 5 mGy or more estimated to be 64% (Table 10). Parameter estimates with confidence intervals for the preferred CML ERR and EAR models are given in Table 11, respectively. The precise form of this model is given in supplementary Table S2 (http://dx.doi.org/10.1667/RR2892.1.S1). Figure 4c and d illustrate the temporal pattern for the Hiroshima ERR for this model as a function

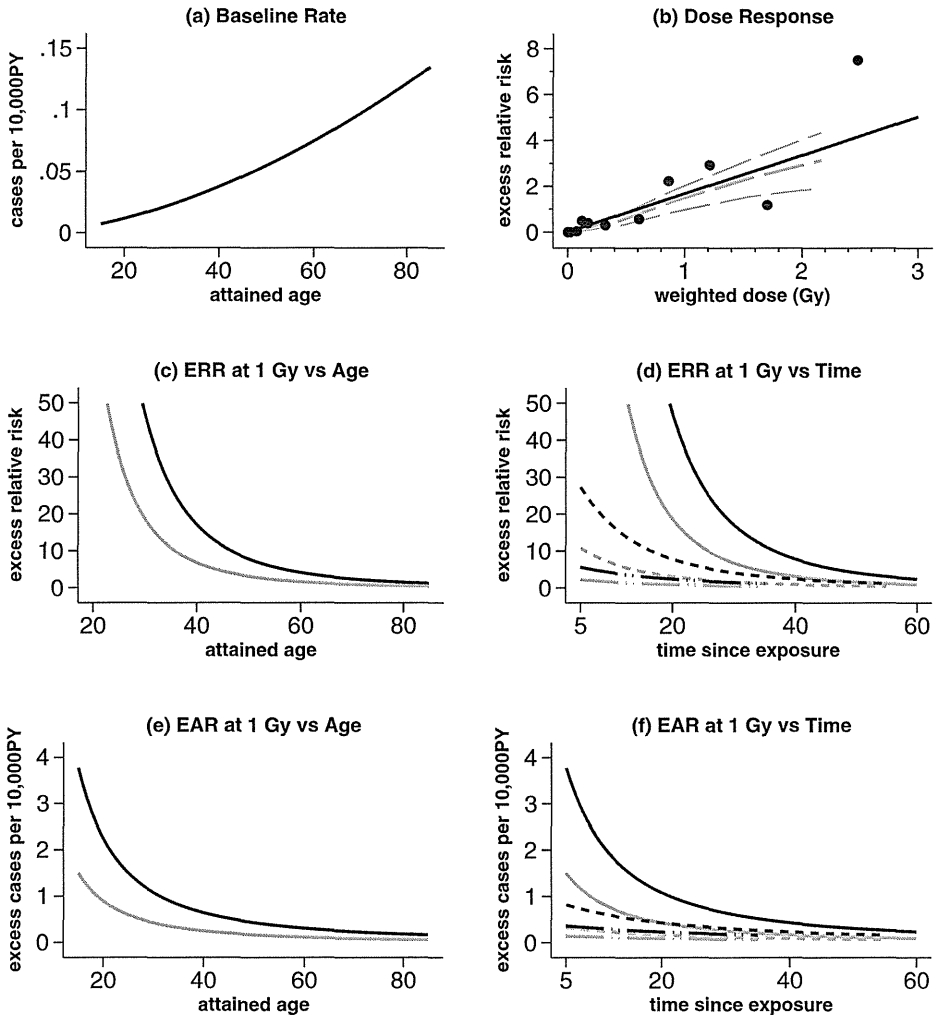

FIG. 3. LSS acute lymphoblastic leukemia risk summary plots. Panel a: shows age-specific Hiroshima baseline rate for LSS cohort members. Panel b: illustrates the radiation dose response based on the ERR model with gender average risks standardized to attained age 70. The solid-black line illustrates the fitted linear dose response. The points are based on a nonparametric dose response model, while the middle-dashed-gray line is a smoothed version of the dose category-specific estimates from the nonparametric fit. The upper- and lower-dashed-gray lines are plus and minus one standard error from the smoothed fit. Panels c and d: exhibit the temporal patterns for men (black line) and for women (gray line) in either city based on the preferred ERR model. Plots (e) and (f) present the temporal pattern for males (black) and females (gray) based on the preferred EAR model. In panels e and f: different line patterns are shown for ages at exposure of 10 (solid line), 30 (dash line) and 50 years (dash-dot line).

of attained age and time since exposure for exposure ages of 10, 30 and 50 years, respectively.

A model in which the ERR varied jointly with age at exposure, time since exposure and city (AIC = 777.7) described the data as well as the attained age, time since exposure and city model described above (AIC = 776.4). However, a model in which the ERR varied with attained age, age at exposure and city fit less well (AIC = 782.0). Parameter estimates and AIC values for these and other alternative models for the CML excess risk are given in supplementary Table S9 (http://dx.doi.org/10.1667/RR2892.1.S2).

In our preferred EAR model, the excess rate depended on city, time since exposure and a gender-dependent attained age effect. The gender-averaged EAR at age 55 after exposure at age 30 was 0.62 cases per 10,000 PY per Gy (95% CI 0.27–1.15). Excess rates for Nagasaki were about 23% of those in Hiroshima ($P = 0.01$). Figure 4e and f show the CML EAR temporal trends by gender and different age-at-exposure groups based on the preferred EAR model. For a given age at exposure, the decrease in the EAR was proportional to time since exposure to the power -1.63 ($P < 0.001$). The attained age effect differed significantly for men and women ($P = 0.01$). For any given time since exposure, the EAR for men exhibited little variation with attained age, decreasing in proportion to attained age to the power -0.20 ($P > 0.5$). Conversely, for women the EAR increased significantly ($P = 0.009$) with

TABLE 8
Observed and Fitted Background and Excess Cases of Acute Lymphoblastic Leukemia by Weighted Bone Marrow Dose Category

Dose (Gy)	Person years	Observed cases	Fitted cases†	
			Background	Excess
<0.005	2,039,093	11	12.0	0.06
–0.1	957,889	8	5.7	1.6
–0.2	201,935	4	1.2	1.6
–0.5	206,749	2	1.3	3.4
–1	117,855	5	0.7	4.0
–2	64,122	5	0.4	4.5
2+	25,761	8	0.1	6.4
Total	3,613,404	43	21.4	21.6

† Estimates based on the preferred linear ERR model described in the text and Table 9 with more details in supplementary Table S2 (http://dx.doi.org/10.1667/RR2892.1.S1).

increasing attained age. This increase was proportional to attained age to the power 2.10. The preferred EAR (AIC = 779.7) and ERR model (AIC = 776.4) described the data about equally well.

Joint Analysis of AML, ALL and CML Dose Response

The results described provide clear evidence of a time-varying radiation dose response for AML, ALL and CML. As noted in the text and illustrated in Figs. 2, 3 and 4, the temporal patterns and shapes of the dose response appear to differ for these three broad leukemia subgroups. We carried out a joint analysis using the methods described in refs. (*4*) and (*35*) to formally examine the evidence for differences in the nature of the temporal patterns and shapes of the dose response for these three subgroups.

When the subgroups are fit with group-specific baseline rates and the linear-quadratic ERR model developed for all leukemias other than CLL or ATL ("common model"), the AIC was 2,848.8. This is considerably larger than the AIC of 2,825.0 obtained using the preferred subgroup-specific models described above. For EAR models, the AIC using the common EAR model was 2,858.1, while the AIC based on the preferred subgroup-specific EAR models was 2,827.5. Although a formal test of statistical significance is not possible, based on a comparison of the differences between the AICs for the common and group-specific models, there is a clear indication of subgroup differences for both the ERR and EAR models.

In the ERR model, there is evidence of significant heterogeneity relative to the common model with regard to variation in the risk with attained age ($P = 0.01$), time since exposure ($P = 0.004$) and city ($P = 0.03$). When the effect modification was allowed to have the form of the preferred model in each subgroup, there was little evidence of significant inter-subgroup variability in the dose-response curvature ($P = 0.14$).

Test for heterogeneity in EAR effect modification relative to the common EAR model indicates some evidence of heterogeneity with regard to gender ($P = 0.04$). After allowing for gender variation, there is evidence of heterogeneity with regard to time-since-exposure ($P = 0.01$) or age-at-exposure ($P = 0.04$) effects. As with the ERR model, there was little evidence of significant inter-subgroup variability in the dose-response curvature ($P = 0.17$).

Table 12 contains estimates of the possible number of radiation-associated excess cases by time period (for all age-at-exposure groups together) based on the preferred ERR models for AML, ALL and CML. The largest number of excess cases was seen during the first 5 years of follow-up. Table 12 also provides information on the within-period distribution of the excess over the three subtypes considered here. It can be seen that, while most of the excess cases in the 1950–1955 period are CML, as time has gone on AML has come to account for most of the excess.

Chronic Lymphocytic Leukemia (CLL)

CLL is rare in Japan. In the previous report, there were only four CLL cases, which were analyzed with the other leukemias. With additional follow-up time, 12 CLL cases

TABLE 9
Preferred Model, Excess Risk Parameter Estimates for Acute Lymphoblastic Leukemia

Risk model	Linear dose coefficient (at 1 Gy)	Gender ratio (F:M)	Attained age (power)
ERR† Female	0.95 (0.23, 3.37)	0.40 (0.14, 0.99)	–3.51 (–5.29, –1.92)
Male	2.40 (0.63, 7.90)		
EAR‡ Female	0.09 (0.03, 0.25)	0.40 (0.14, 0.99)	–1.81 (–2.56, –1.08)
Male	0.23 (0.07, 0.58)		

† The preferred ERR model is linear in dose with log-linear effect modification depending on log (attained age) and gender. The baseline model parameters and explicit details about the dose effect modification term are given in Table S2 in the supplementary material (http://dx.doi.org/10.1667/RR2892.1.S1). Supplementary Table S8 (http://dx.doi.org/10.1667/RR2892.1.S2) presents information on alternative ERR models. The dose coefficients describe the ERR at 1 Gy at age 70.

‡ The preferred EAR model is linear in dose with log-linear effect modification depending on log (attained age) and gender. The baseline model parameters and explicit details about the dose effect modification term are given in Table S2 in the supplementary material (http://dx.doi.org/10.1667/RR2892.1.S21). Supplementary Table S8 (http://dx.doi.org/10.1667/RR2892.1.S2) presents information on alternative EAR models. The dose coefficients describe the excess cases per 10,000 person years at 1 Gy at age 70.